AD NUMBER
AD816133
LIMITATION CHANGES
TO: **Approved for public release; distribution is unlimited.**
FROM: **Distribution authorized to U.S. Gov't. agencies and their contractors; Critical Technology; JUL 1967. Other requests shall be referred to Air Force Rocket Propulsion Laboratory, RPPR/STINFO, Edwards AFB, CA 93523. This document contains export-controlled technical data.**
AUTHORITY
AFRPL ltr, 27 Oct 1971

SPECTROMETRIC EVALUATION OF METAL CONTAINING FUELS

William H. McLain
Robert W. Evans

University of Denver
Denver Research Institute

FINAL TECHNICAL REPORT 558-6608-F

July 1967

[redacted]

Air Force Rocket Propulsion Laboratory (RPCL)
Edwards Air Force Base, California

NOTICES

SPECTROMETRIC EVALUATION OF METAL CONTAINING FUELS

William H. McLain
Robert W. Evans

FOREWORD

This Final Technical Report was prepared under Air Force Contract Number AF 04(611)-10782 and summarizes the work accomplished under the subject contract from June 1965 to June 1966. The work was performed under the direction of the Air Force Rocket Propulsion Laboratory (RPCL), Edwards Air Force Base, California, with Capt. W. H. Summers, acting as Project Officer. Denver Research Institute personnel responsible for the work include William H. McLain and Robert W. Evans.

The authors wish to express appreciation to Mr. Ralph E. Williams and Mr. Larry D. Cameron for their considerable contributions to one or more phases of this research program.

This technical report has been reviewed and is approved.

W. H. Ebelke, Colonel, USAF
Chief, Propellant Division

ABSTRACT

The spectral characteristics of high temperature Hybaline B-3 fueled combustion reactions are reported. Data were obtained for Hybaline B-3 augmented hydrogen-oxygen, deuterium-oxygen, acetylene-oxygen, and air diffusion flames under conditions simulating rocket test firings. Major features of the emission spectra are outlined for the ultraviolet, visible, and infrared regions. Sufficient specific emission is available to indicate the feasibility of determining changes in the species concentrations and flame temperatures as functions of changes in O/F ratios and other major rocket parameters.

High temperature Hybaline B-3 flame studies indicate that sufficient selective emission occurs in the visible region to allow the detection and analysis of the vapor phase combustion product $BO_2(g)$. In addition, in the infrared region, prominent spectra have been observed which are specific in character. These spectra have been correlated with emission from water, a combination of carbon monoxide and carbon dioxide, and selective emission peaks in the 5.0 to 6.0 micron region which are tentatively attributed to HBO_2 and BO. Sufficient resolution is available in both the visible and infrared regions to allow analysis of relative peak intensities as time-resolved functions. The emission spectra of this system in the ultraviolet region consisted mainly of the OH bands. No evidence of emission from any beryllium species was observed in these burner studies. The spectrographic techniques developed on this program show promise as possible methods for determining the "real time" kinetic behavior of Hybaline B-3 fueled rocket combustion gases.

PREVIOUS PAGE WAS BLANK, THEREFORE WAS NOT FILMED.

TABLE OF CONTENTS

LIST OF FIGURES

LIST OF FIGURES (Continued)

LIST OF TABLES

I. INTRODUCTION

The objective of this research program was to determine the feasibility of using spectroscopic methods for the purpose of evaluating the extent of thermal and chemical equilibrium within a methylamine beryllium borohydride (Hybaline B-3) fueled rocket plume. This objective was accomplished by a detailed analysis of the species present in the flame of a small burner which simulated rocket plume conditions. Emphasis was placed on the identification of the species which emitted enough discrete radiation to provide a basis for a possible concentration analysis. Such concentrations are dependent on the mixture ratios (O/F) and the pressure levels at which the combustion occurs, therefore the relative spectral intensities can be correlated with theoretical shifting or frozen equilibrium calculations. From a detailed analysis of the emission characteristics of the combustion plume, an evaluation of the critical physical and chemical processes important to the establishment of equilibrium can be performed.

In addition, wet chemical analyses of the products of reaction were selectively used to correlate the observed spectral data. Also, chemical analyses were used to identify intermediate chemical species which exist in the Hybaline B-3 flame. Based on these studies, a model of the pyrolysis mechanism is proposed. It is concluded that emission spectroscopy can provide useful data relative to the high temperature thermochemistry and kinetics of boron-fueled rocket-exhaust plumes. The major results of this research program are summarized in the following sections.

II. EXPERIMENTAL PROGRAM

A. Introduction

The approach used in this research program was to perform a preliminary series of studies to obtain relative spectral emission intensities. For these studies a burner technique was developed to simulate a rocket combustion chamber. Using this burner, boron and beryllium containing powders or compounds could be added to preselected and carefully controlled base flames. This portion of the program served two primary purposes. One purpose was to calibrate instrumentation under closely controlled experimental conditions. The second purpose was to obtain a qualitative documentation of the relative intensity levels for important emitting species using the actual equipment and techniques which would be applied later to propellant combustion studies. Following the calibration and preliminary investigation studies, experimental work using Hybaline B-3 flames was initiated. Because of the toxicity of the combustion products formed during this reaction, considerable emphasis was placed on developing safe operating procedures and facilities. A brief outline of the techniques employed and comments relating to the handling characteristics of Hybaline B-3 is given in Appendix II.

B. Burner for Combustion Studies

While several burner configurations were used for these studies, most of these were modifications of the burner shown in Figure 1. It is essentially a modified cutting torch in which the base flame was either hydrogen-oxygen or acetylene-oxygen. To this base flame, boron and beryllium powders or compounds could be added as necessary to provide the desired mixture ratios. The liquid Hybaline B-3 could not be added directly in this burner because of extensive plugging at the orifices. To minimize plugging it became convenient to add the Hybaline B-3 separately in an atomized liquid form. For this purpose a standard one on one impinging jet atomizer was used. The carrier gases used were either helium or argon in order to provide an inert system. Two principle injection techniques were used. A cross axial injection position of the atomization stream was used to simulate short, flame residence times of hybaline droplets. An on-axial placement of the injector was used to simulate a longer flame residence time.

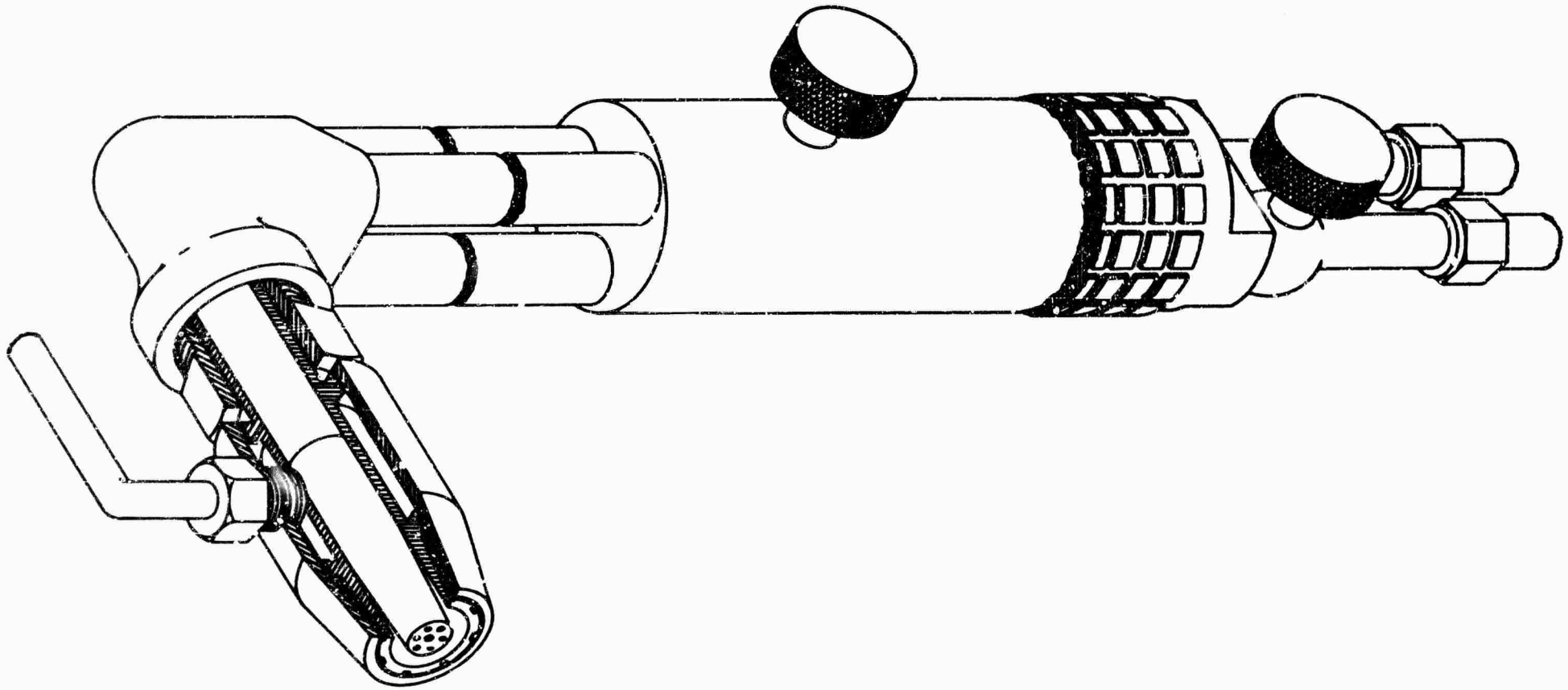

Figure 1. Burner for Metal Powder Combustion Studies

Typical arrangements of the hybaline injector system are shown in Figures 2 and 3. Flow rates were monitored using standard flow meter techniques for the gaseous flows necessary for the base flame, and time-displacement methods for the neat propellant.

While in operation, the injector was placed as close as possible to the combustion zone. However, some difficulty was encountered even in an argon shrouded atmosphere with flash back to the atomizer. The result of such flash back was to initiate a stable flame held on the injector. When this occurred, extensive plugging of the orifices took place, which reduced the fuel flow rates. To avoid this problem the injector assembly was placed at varying distances from the combustion zone depending on the run conditions. Thus the entire reaction was made to occur within a closely defined area of observation.

All the results presented in this report were obtained at ambient Denver pressure (approximately 640 torr). Toward the end of the contract period a pressure vessel was fabricated so that the burner could be operated at high pressures. However, experimental difficulties were encountered which precluded the acquisition of data at higher than ambient pressures.

C. Spectral Analysis of Radiation

Combustion processes are usually unsteady so an instrument which scans a spectral region rapidly provides the most useful information concerning the spectral distribution of radiation from a flame or rocket plume. But, in general, the spectral resolution is low for most rapid scan spectrophotometers. Therefore, it is necessary to get complementary, time integrated data in order to correctly interpret the results from the rapid scan instrument.

Four instruments were used for obtaining the spectral distribution of the radiations produced by the burner plume.

1. Perkin-Elmer Model 108 Rapid Scan Monochromator. This instrument was used for obtaining spectral information in the visible and infrared spectral region. For this program a nominal scan time of approximately 300 milliseconds was used. Adequate resolution was obtained in the infrared region; however, the relatively low dispersion of this instrument tends to limit its usefulness in the visible and ultraviolet regions to studies of band intensities.

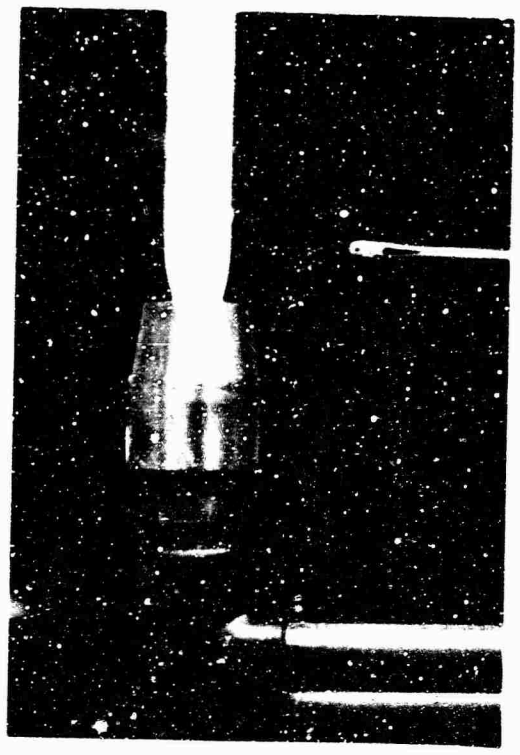

Figure 2. Typical Cross Axial Injection for Hybaline B-3 Fuels

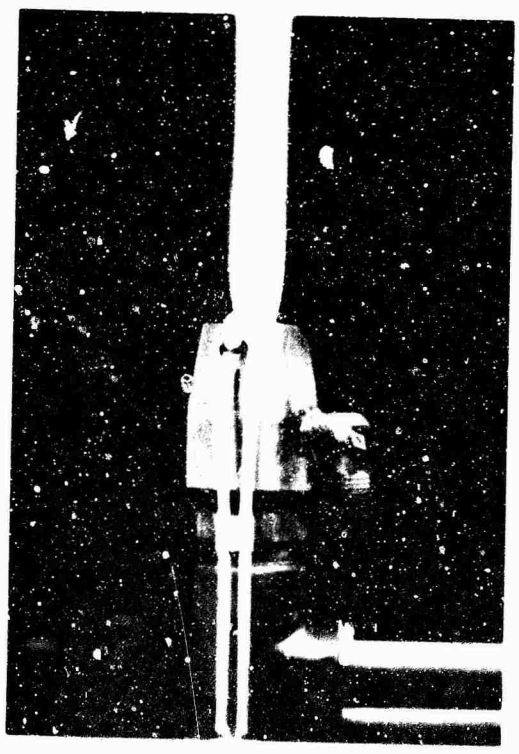

Figure 3. Typical Axial Injection Burner Configuration for Hybaline B-3 Fuels

2. CINE Framing Spectrograph. This instrument has a large aperture so that reasonable time integrated spectral data can be obtained from relatively low intensity sources in the visible and ultraviolet spectral region. However, because it has a relatively low dispersion in the visible, its usefulness is limited. Framing rates greater than 1000 frames per second can be obtained from this instrument.

3. Bausch and Lomb Grating Spectrograph. This instrument was used mainly to obtain relatively high resolution, time integrated spectra in the visible and ultraviolet regions (3000 Å to 8000 Å). The principle problem with this spectrograph is its inherent slowness caused by overall aperture of about f22.

4. Hilger Prism Spectrograph. This instrument was also used to obtain time integrated spectra in the visible and ultraviolet spectral region. It is relatively fast (approximately f4.5), and because of its quartz prism, had very good resolution in the ultraviolet region.

D. Experimental Results

Typical spectra obtained with these instruments are shown in Figures 4 through 14.[1] In Figures 4 and 5 the background emission is given for a hydrogen-oxygen flame and an acetylene-air flame. In Figure 4 the major structure consists of water emission at (2.7μ). To the far right hand side, the spectrum from a 6.25 hydroxyl band is observed. A comparison of this spectrum with the Hybaline B-3 augmented flame shows a downward spectral shift to a peak at about 5.4 - 6.0 microns. In Figure 5 the structure in the acetylene-air flame consists of blackbody emission from carbon soot, and a combined CO-CO_2 peak at about 4.5 microns. As the temperature increases, the blackbody radiation will tend to shift its peak value to higher frequencies although the absolute intensity will increase at all wave lengths. Since relative peak heights are used by varying the amplifier gain, corrections can be made to account for the blackbody background.

An emission spectrum from a Hybaline B-3 augmented hydrogen-oxygen flame is shown in Figure 6. In this figure the major peaks correspond to water; a combined CO, CO_2 band, and unidentified bands

[1] Because of its relatively low dispersion, no time resolved spectra taken with the CINE spectrograph are included.

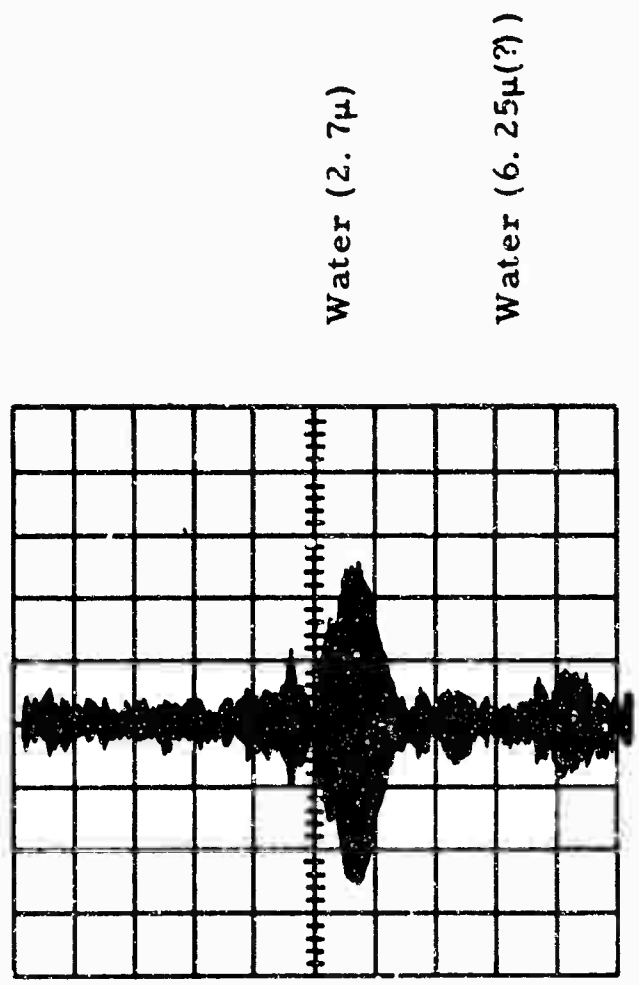

Perkin Elmer Rapid Scan

Figure 4. A Typical Background Spectrum in the Infrared Region Using a Hydrogen-Oxygen Flame

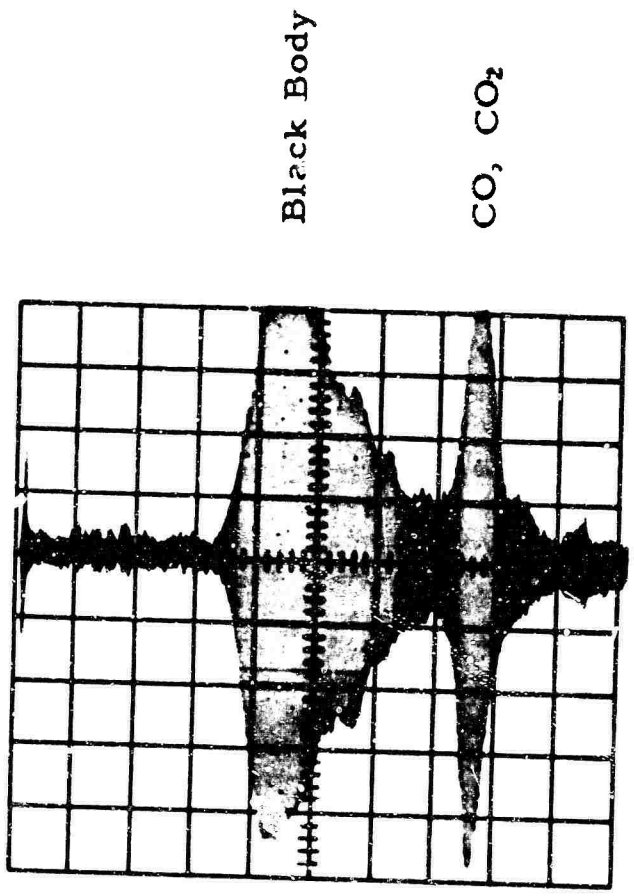

Perkin Elmer Rapid Scan

Figure 5. A Typical Infrared Spectrum Obtained from an Acetylene-Air Diffusion Flame

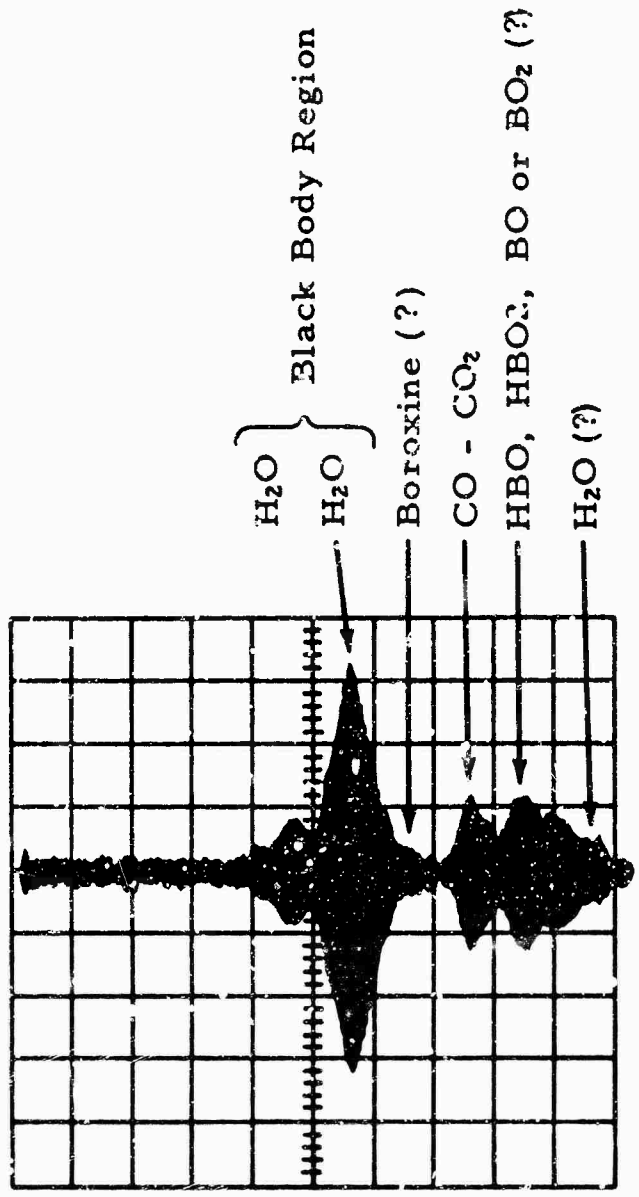

Perkin Elmer Rapid Scan

Figure 6. A Typical Spectrum in the Infrared Region for a Hybaline B-3 Augmented, Hydrogen-Oxygen Flame

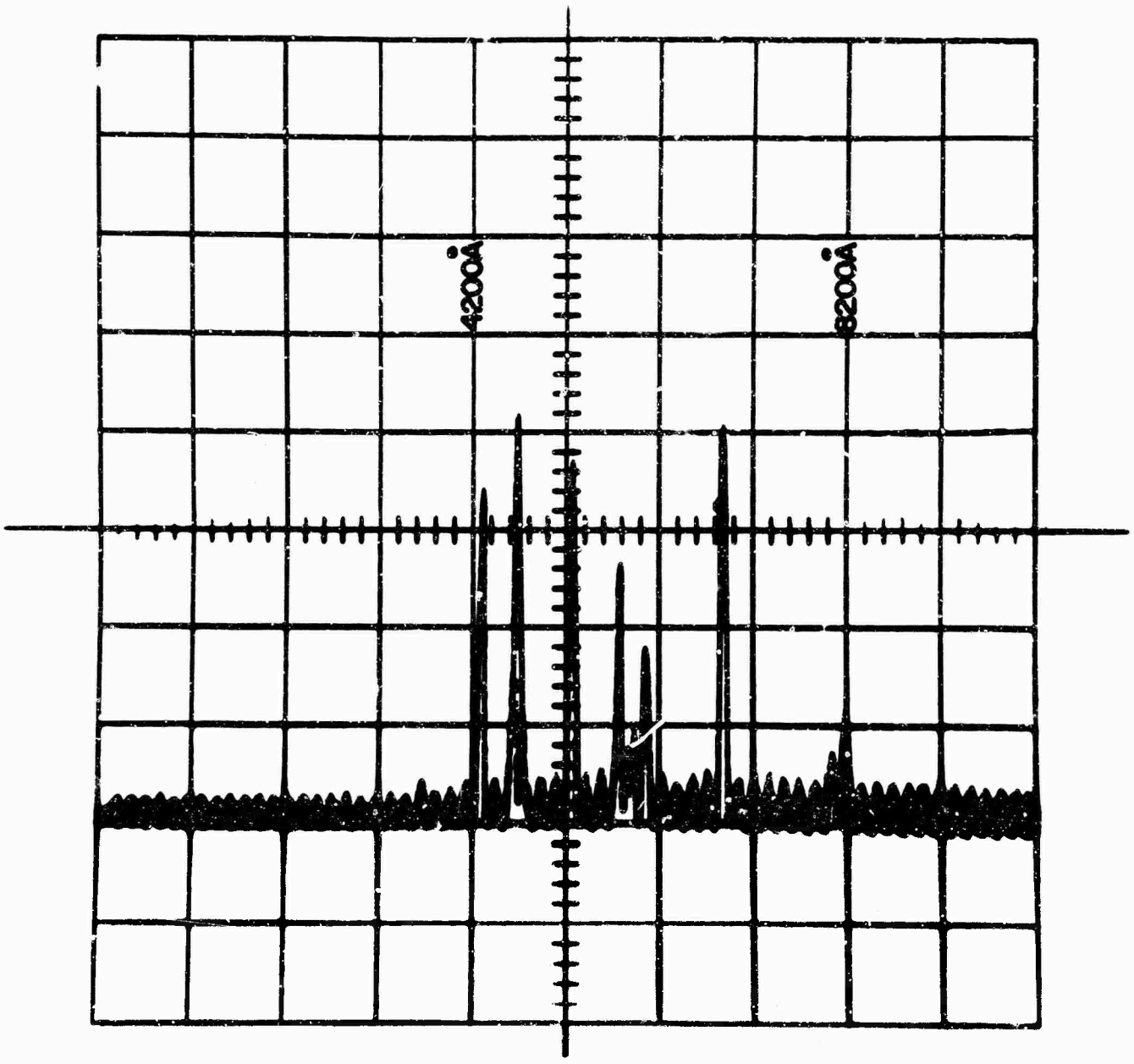

Figure 7. Spectral Resolution Capability of the Perkin-Elmer 108 Rapid Scan Spectrophotometer in Visible Region

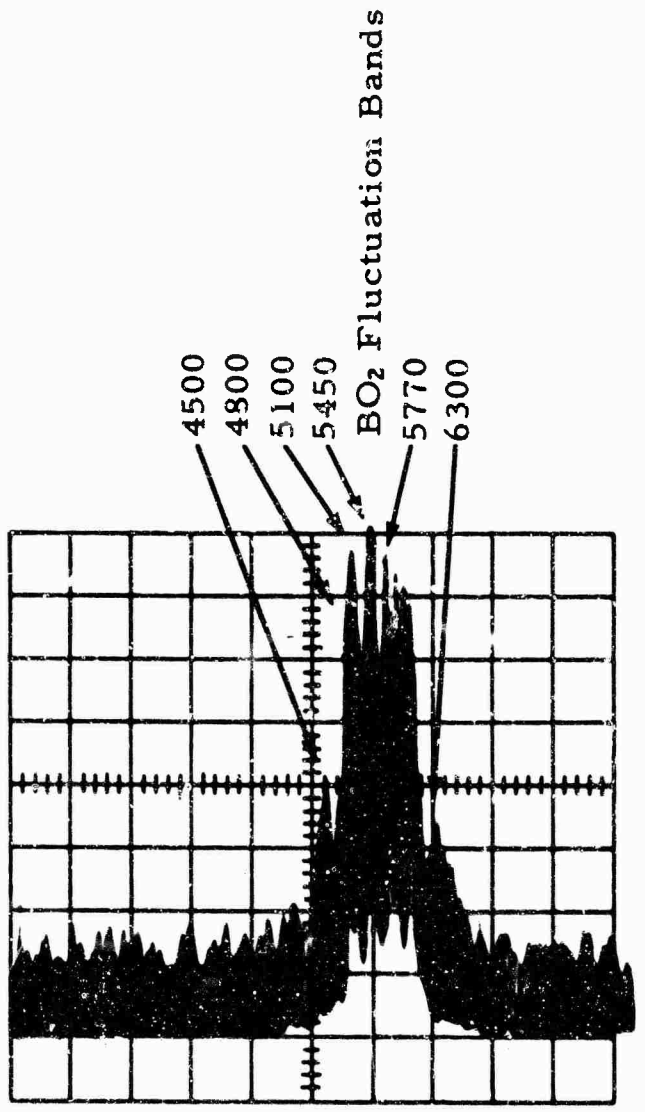

Perkin Elmer Rapid Scan

Figure 2. A Typical Spectrum in the Visible Region Using the Perkin-Elmer Scanning Spectrometer

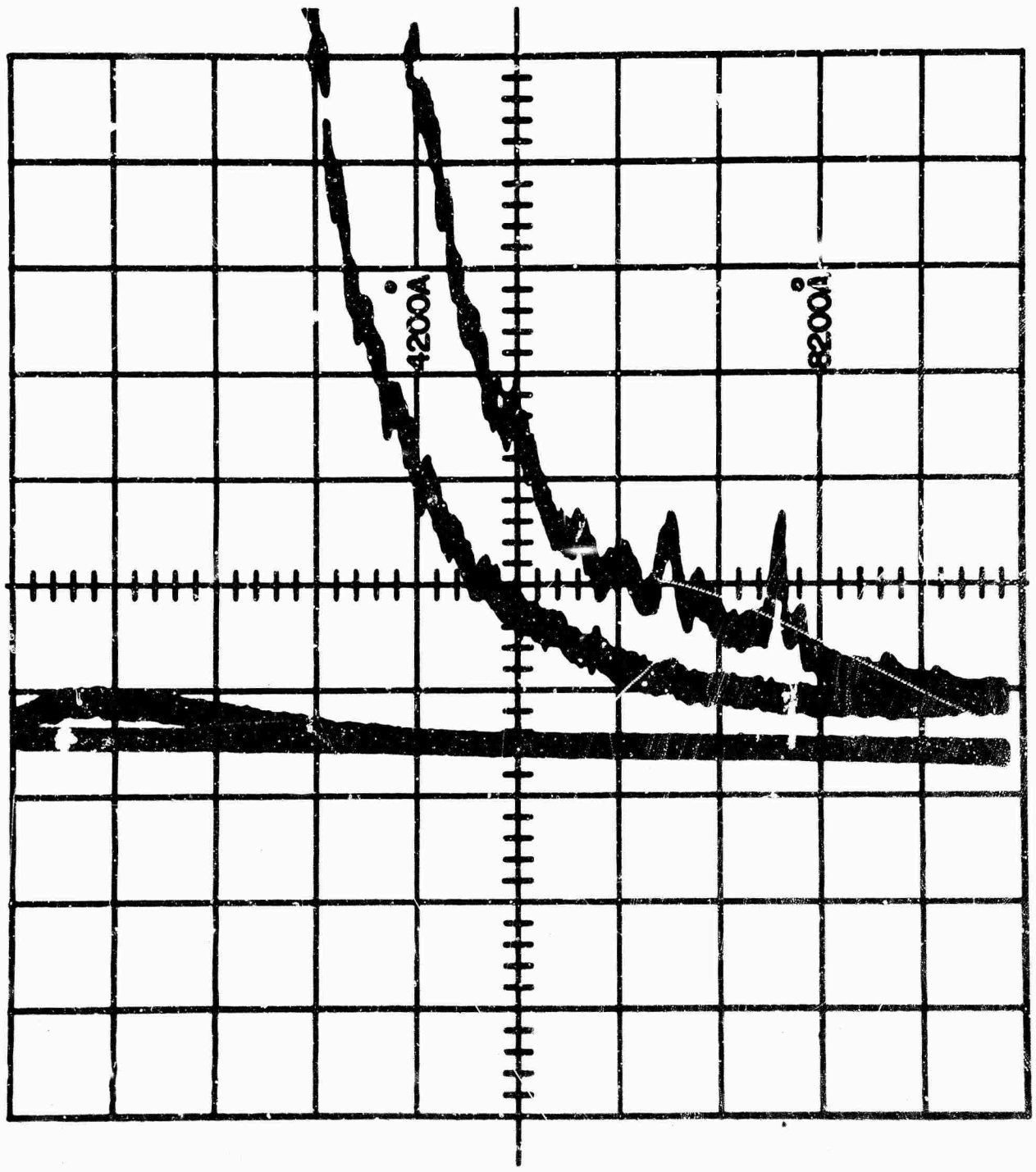

Figure 9. Spectral Characteristics in the Visible Region of Radiation from a Pyrotechnic Mixture

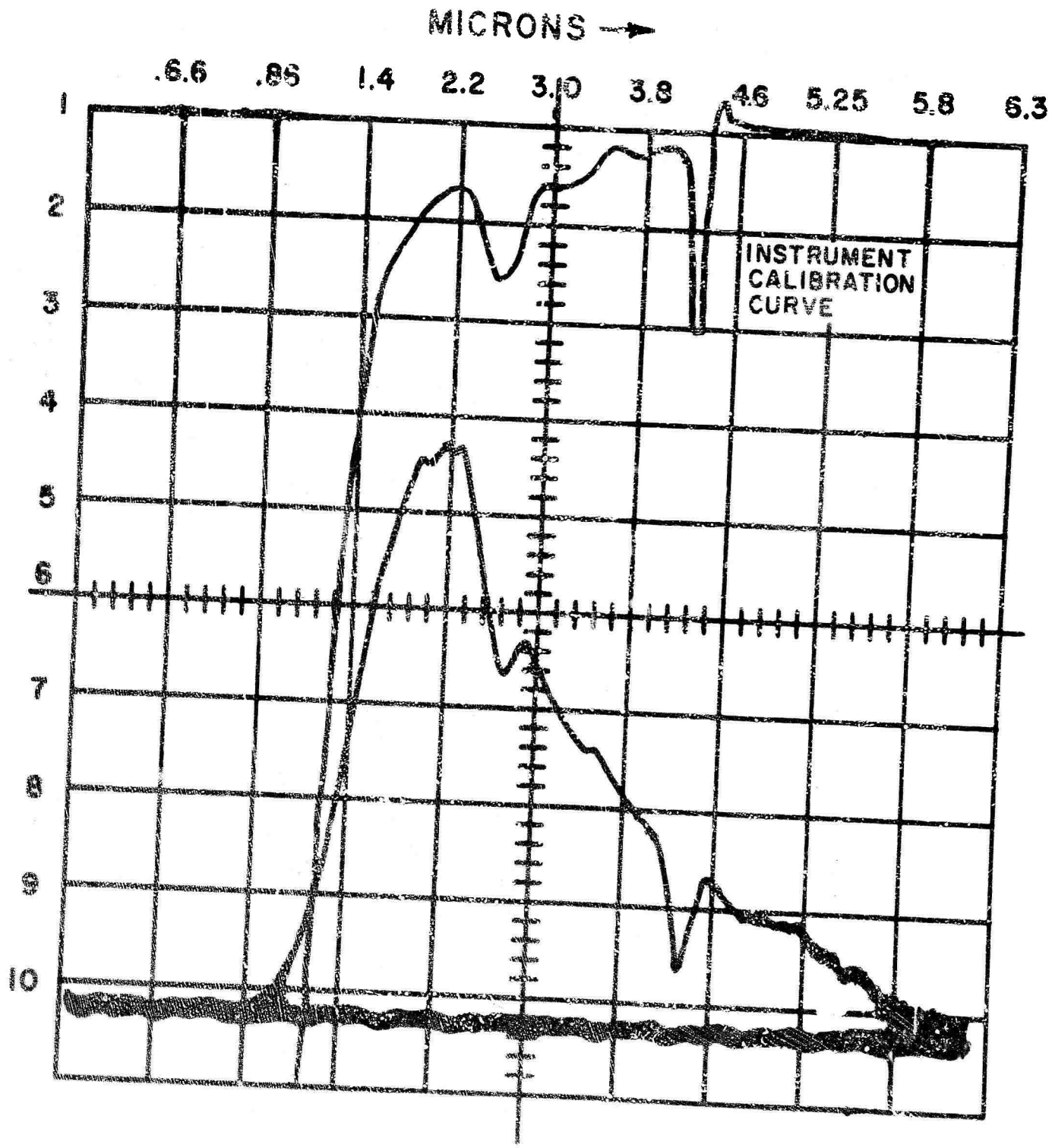

Figure 10. Infrared Radiation from a Boron Loaded Pyrotechnic Mixture

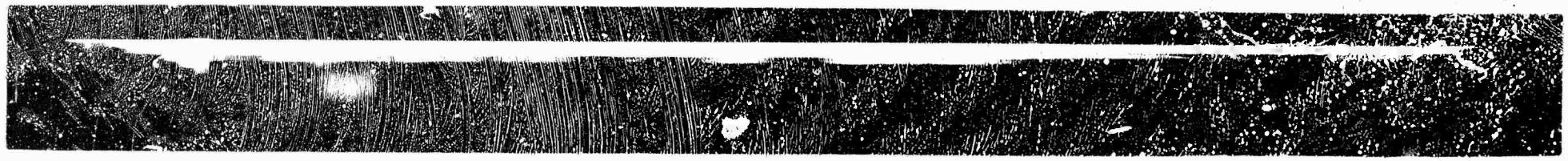

Figure 11. Calibration Spectrum of Boron Oxide

Figure 12. Calibration Spectrum of BeO

High Temperature Fuel Rich Oxygen Acetylene-Hybaline B-3 Flame
Thirty Seconds Duration with Step Density Filter - B & L Spectrograph

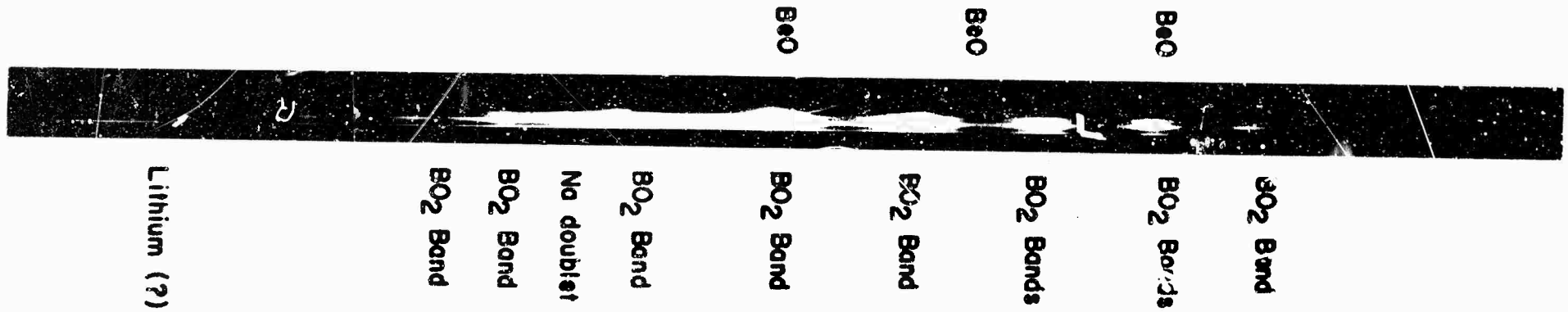

High Temperature Neutral Flame-Acetylene-Oxygen Hybaline B-3
Thirty Seconds Exposure with no Step Density Filter - B & L
Spectrograph BeO(g) Emission Present but Obscured by BO_2
Fluctuation Bands

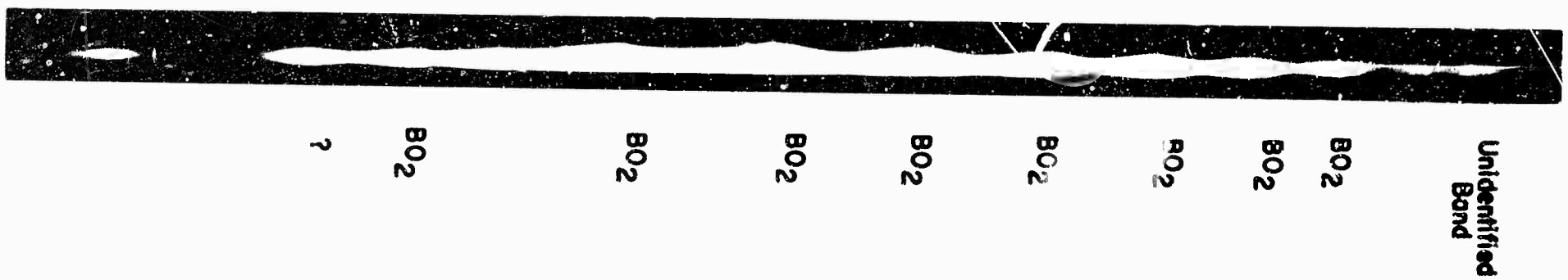

Figure 13. Spectra from Hybaline B-3 Augmented Oxygen-Acetylene Flames

Figure 14. Hybaline B-3 - Air Flame - Bausch & Lomb Grating Spectrometer 45 Second Exposure

at about 5.4 and 5.9 - 6.1 microns. The assignment of this latter peak is not clear but could be interpreted as a H-OBO stretching mode. This oscilloscope tracing clearly shows pronounced structure in the infrared region. Although the flame is somewhat dilute, blackbody emission from incandescent particles would probably not be high enough to mask out this structure. This is particularly true for the radiation at 5.9 microns where the blackbody radiation is relatively weak. The spectral resolution of the Perkin-Elmer 108 in the visible region is indicated by Figure 7. This spectrum was obtained using a mercury arc calibration lamp. A Perkin-Elmer 108 spectrum showing the BO_2 fluctuation bands is shown in Figure 8. In this figure the structure consists of BO_2 fluctuation bands in the visible region.[2] There is not sufficient resolution here to allow quantitative data although some use might be made for qualitative work. The B & L grating spectrometer is better suited for this analysis if exposure times of the order of 10 seconds can be tolerated.

Figures 9 and 10 show results from a boron loaded pyrotechnique mixture. Some of the boron fluctuation bands appear in the visible region (Figure 9) but are of only gross qualitative interest. In Figure 10 the infrared radiation from a similar mixture is shown together with the associated calibration curve for that region.[3]

Calibration spectra for boron and beryllium oxides were obtained by arcing the metals in an oxygen atmosphere, using the Bausch and Lomb grating spectrometer. They are shown in Figures 11 and 12. These spectra are of relatively high resolution and considerable structure is present. High temperature Hybaline B-3 augmented acetylene-oxygen spectra are shown in Figure 13. The beryllium oxide bands are not discernable over the BO_2 fluctuation bands under the conditions of these experiments. A similar spectrum for a hybaline-air flame is shown in Figure 14. Again only the BO_2 fluctuation bands are observed in emission.

---

[2] Based on work with the B & L grating instrument, some of this represents overlap and a portion is attributable to the background noise in the system. This data would be useful for integrated band studies, but is limited if specific bands or lines are to be closely studied.

[3] This calibration includes the absorbance caused by windows and optical attenuation in the reaction chamber and associated instrumentation. The value of the ordinate at a particular wavelength is the value by which the observed output (lower) curve should be multiplied.

The Hilger spectrograph covers an effective spectral range between 2000 Å and 9000 Å. However, for these studies, because of its optical design, it is most useful in the 2000 to 4000 Å region. A calibration spectrum showing the mercury lines is given in Figure 15 together with spectra for hybaline-air diffusion flames. A relatively firm assignment of the H atom in absorption was made and this was somewhat unexpected. The spectra obtained from a series of Hybaline B-3 augmented hydrogen-oxygen and deuterium-oxygen runs is shown in Figure 16. An enlargement of the OH emission structures in the 3000 Å region is given in Figure 17.

E. Discussion of Results

For Hybaline B-3 fueled burner plumes, useful information can be obtained in three spectral regions; the infrared, the visible, and the ultraviolet. Major species observed in emission are listed in Table I. More details concerning the prominent features in each spectral region are given in the following sections.

TABLE I. SPECIES OBSERVED IN THE EMISSIONS OF HYBALINE B-3 FLAMES

Ultraviolet Spectral Region[4]	OH
Visible Spectral Region	BO_2 H_2O H_2O
Infrared Spectral Region	CO_2 - CO HBO_2 HBO BO

1. Infrared Region

Prominent spectra have been observed in the infrared region which are specific in character, and are probably associated with emission from water, a combination of carbon monoxide and carbon dioxide, and two unidentified selective emission peaks in the 5.4 and 5.9 micron regions. These latter peaks may be attributed to HBO,

[4] No beryllium or beryllium oxide bands were observed in the emission from Hybaline B-3 augmented flames.

Hybaline B-3 - Air Diffusion Flame 80 Second Exposure - BO_2 Fluctuation Banks in Emission - H Atom plus Other Structure in Absorption. Crumpled Aluminum Foil Reflector ~ 0.010 Slit.

Hybaline B-3 - Air Diffusion Flame 200 Second Exposure - BO_2 Fluctuation Bands in Emission - No Discernable Absorption. No Reflector ~ 0.005 Slit

Calibration Spectrum for Above Using Hg Quartz Lamp

Figure 15. Spectra Obtained with the Hilger Spectrograph

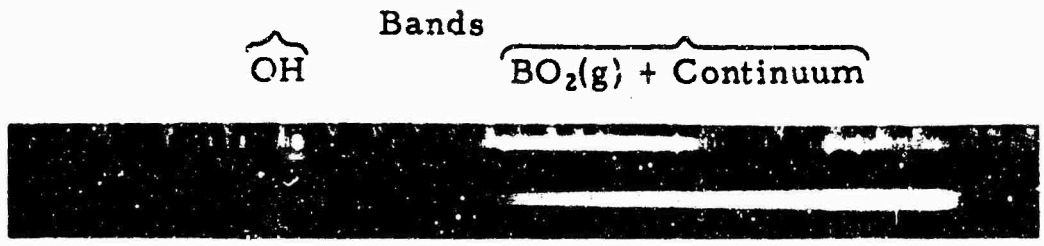

a. Ultraviolet spectra from Hybaline B-3 augmented hydrogen-oxygen flame studies. Time integrated exposures of 40 and 30 seconds.

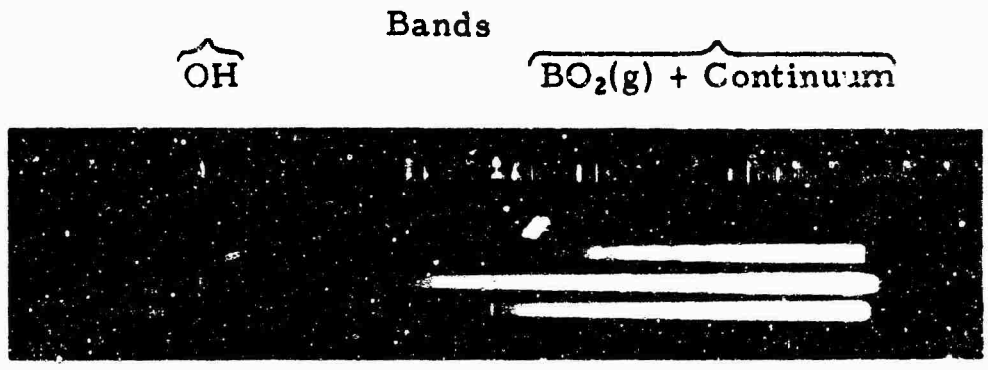

b. Ultraviolet spectra from Hybaline B-3 augmented hydrogen-oxygen flame studies. Mixture ratios are varied from fuel-rich to fuel-lean.

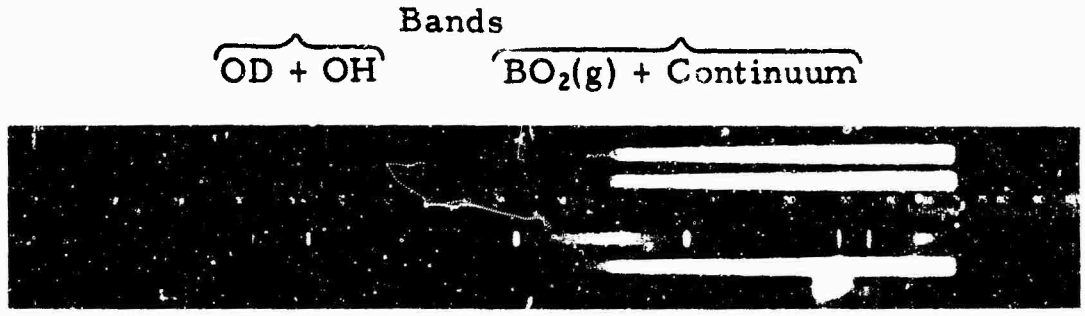

c. Ultraviolet spectra of Hybaline B-3 augmented deuterium-oxygen flames. Mixture ratios are varied from fuel-rich to fuel-lean with the OH and OD bands prominent. Isotropic shifts are readily observed verifying assignment of bands.

Figure 16. Hybaline B-3 Augmented Flame Studies Showing Spectra in the Ultraviolet Region

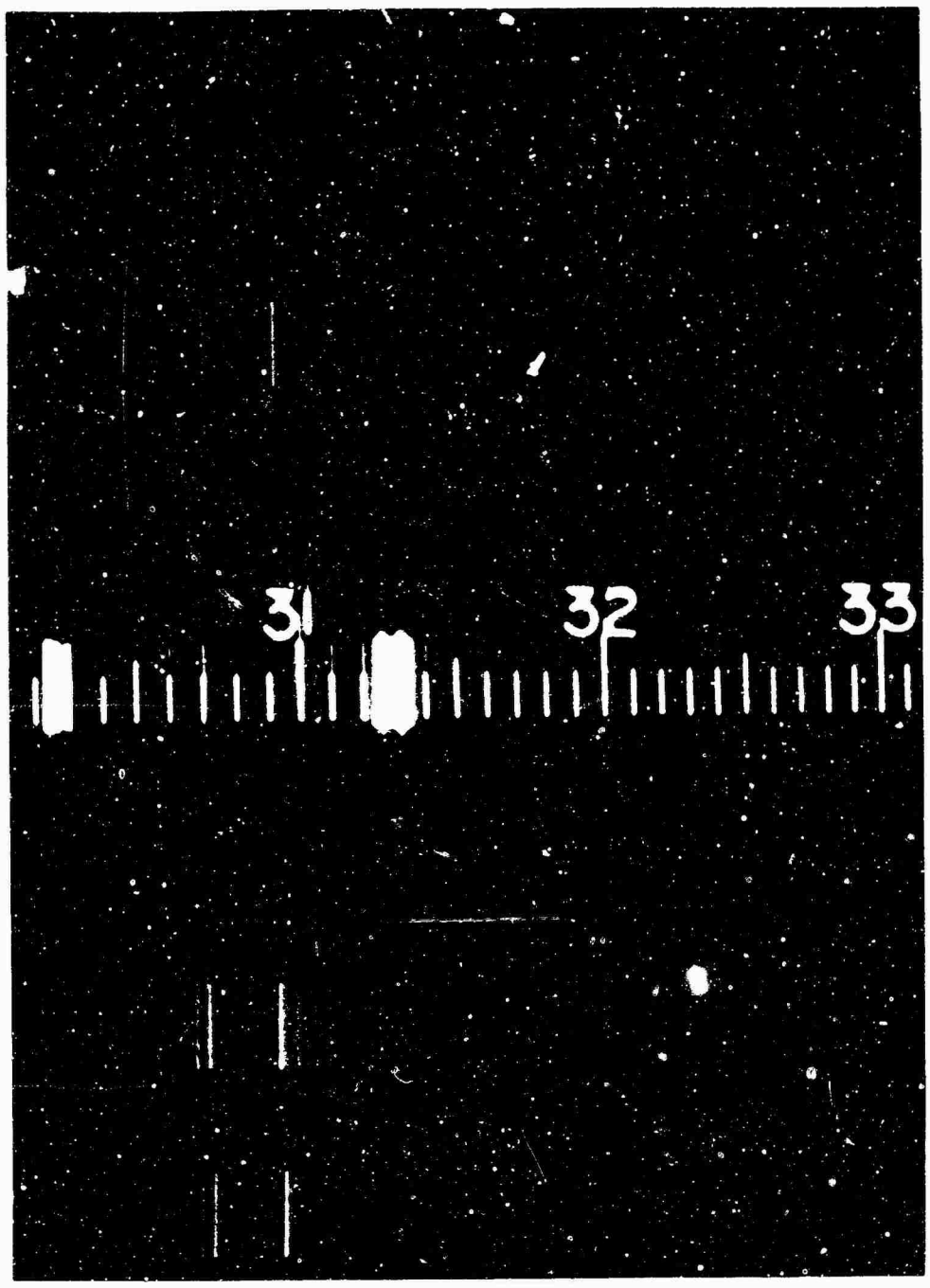

Figure 17. Fine Structure of OH Emission Observed in the 3064 to 3300 Å Ultraviolet Region for Hybaline B-3 Augmented Hydrogen-Oxygen Flame

HBO_2 or BO. Sufficient resolution is available in both the visible and infrared spectral regions to allow analysis of relative peak intensities. These intensities vary with changes in combustion product concentrations caused by varying the O/F ratios and therefore are suitable for determining the "real time" kinetic behavior of these species. The precision of measurement in the infrared region is adequate for determining relative species concentrations as time resolved functions using a scanning rate of about one third second per scan covering the spectral region from one micron through about 6.3 microns. It is probable that satisfactory resolution could be obtained with scan times as low as 10 milliseconds. This capability should enable selected rocket phenomena (e.g., chugging) to be related to specific changes in the concentrations of important combustion products.

2. Visible Spectral Region

As has been indicated, the major structure in the visible spectral region consists of the "BO_2 fluctuation" bands. These bands are a series of thirteen bands ranging from 4075 to 6810 Å which have closely spaced individual lines and broad maxima. There is some discernible structure to these bands with, perhaps, sufficient intensity to be able to use them for analytical spectroscopy. The major difficulty in their use for this purpose is the existence of a broad underlying continuum. The background shift is shown in a microdensitometer tracing in the region of the sodium lines, Figure 18. A tracing of two BO_2 bands, shown in Figure 19, indicates the amount of structure present. Because the general continuous background is less at the shorter wavelengths, these bands may be more useful than those of greater intensity for boron reaction rate studies. Quantitative data may possibly also be obtained using the "bottom" of these bands.

3. Ultraviolet Spectral Region

Using a Hilger quartz prism spectrograph, studies were made of the spectral characteristics of Hybaline B-3 augmented hydrogen-oxygen flames in the ultraviolet region. This spectrograph has a reciprocal dispersion of 5 Å per millimeter at 2100 Å which increases to 20 Å per millimeter at about 4500 Å. The principle spectral features observed with this spectrograph include the BO_2 fluctuation bands in the visible region from 4000 to 6500 Å, together with a series of OH bands starting at about 3060 Å. The BO_2 fluctuation bands are of much greater relative intensity. In the region between 6500 Å and 3300Å a

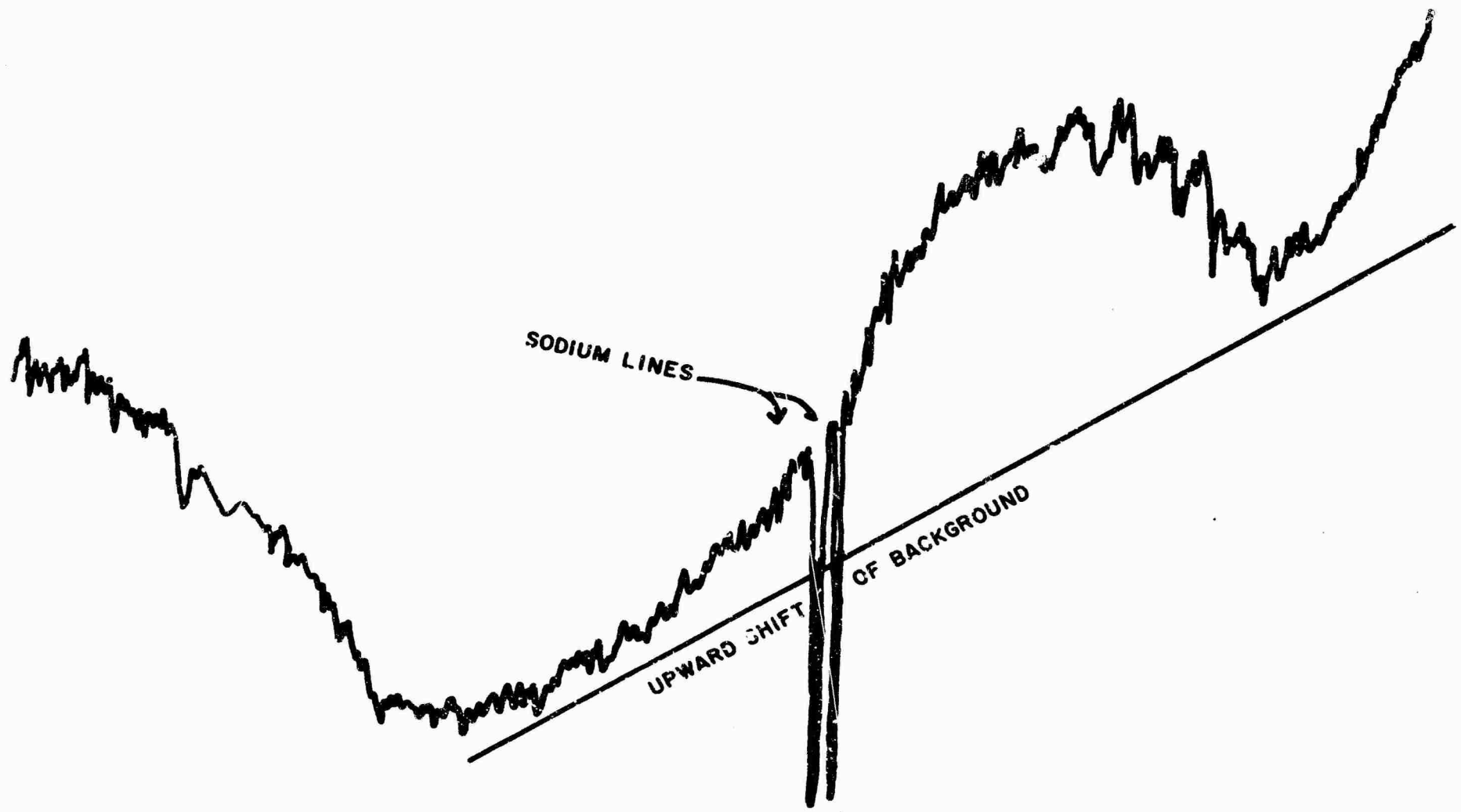

Figure 18. A Typical $BO_2(g)$ Fluctuation Band Superimposed on the Background Continuum

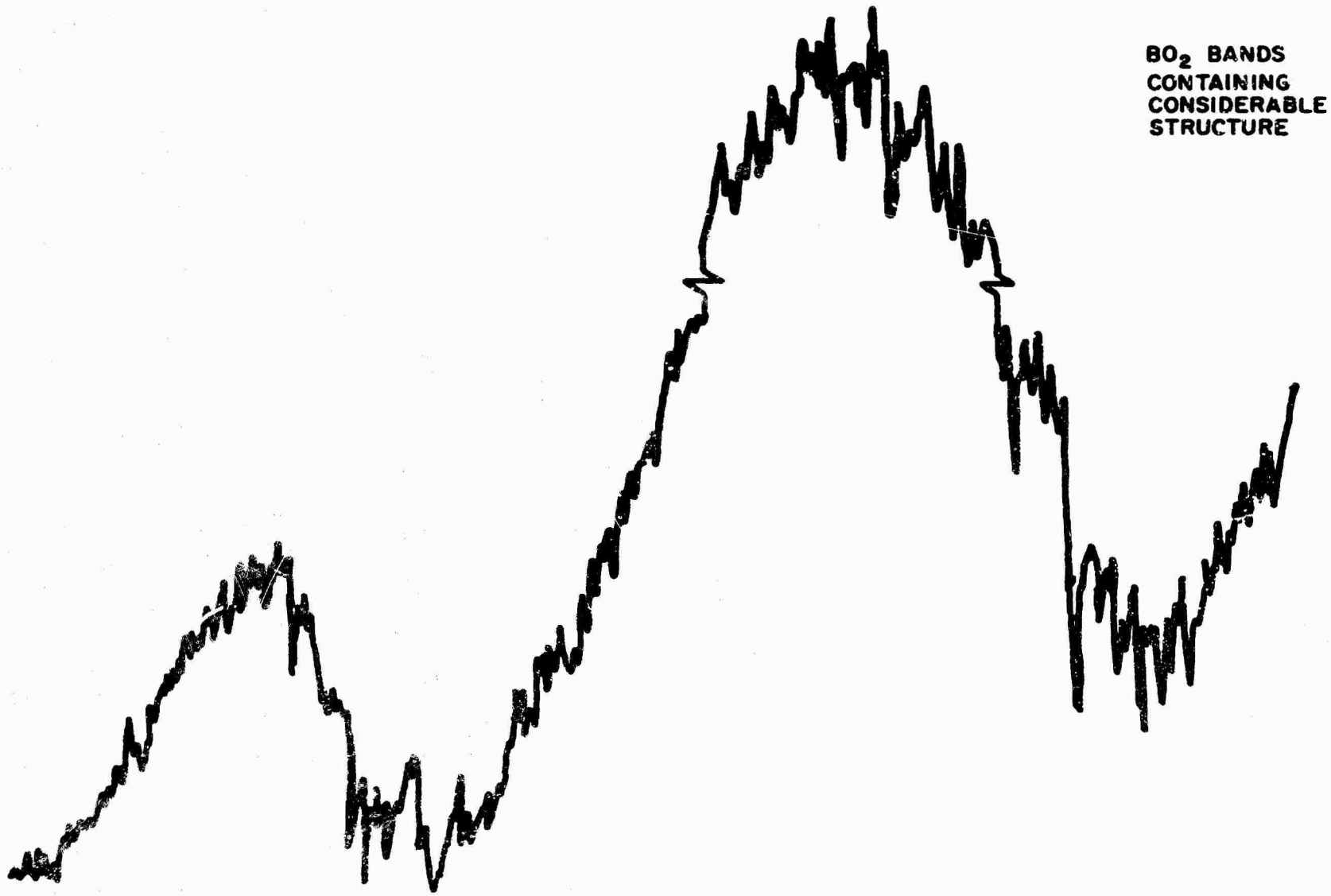

Figure 19. Fine Structure of a Typical $BO_2(g)$ Fluctuation Band Head

continuum background emission is also observed. This continuum cuts off at different wavelengths, depending on the fuel-oxidizer ratios, and a direct correlation exists between the observed cut off region and the calculated flame temperature. This behavior indicates the continuum is due to grey body emission. Because of the low dispersion of the instrument in the visible region, only a limited amount of line structure can be observed in the BO_2 fluctuation bands. That line structure which is observed may possibly be correlated with contaminate species (e.g., FeO) originating from the burner and/or flow lines. The observed band structure originating at 3067 Å degrades to the red. These bands consist of a series of lines with a band head at 3067 Å and another at 3090 Å. Although it may be possible that some of this structure represents emission corresponding to the BO(g) bands, the main structural features correspond to the reported OH band spectra in this region. In these bands, there is sufficient detail to provide independent measurements of flame temperature from observation of the relative intensity distributions.

Typical spectra in the ultraviolet region have been shown in Figures 15, 16, and 17. These spectra represent different O/F ratios of oxygen and hydrogen to which Hybaline B-3 is added. The OH bands in emission are readily observed. Because of partial plugging of the hybaline injector nozzle, the exact Hybaline B-3 fuel rate was not accurately determined, but for most flow conditions, this value was approximately 5 cubic centimeters per minute. The film used for this study was Eastman Kodak Linagraph Shellburst.

An additional series of tests were performed using a deuterium-oxygen flame. Spectral shifts are apparent in the region associated with the bands at 3090 Å. No major shift was observed in the BO_2 fluctuation band structure although some small differences were observed which further confirms the assignment previously made. Because of limited resolving power in the region of the fluctuation bands, an analysis of the fine structure in this region was not attempted.

No spectral emission was observed which could be associated with the Be or BeO species. The lack of Be and BeO spectral emission may indicate that the attainment of equilibrium concentration of BeO is in some manner inhibited under these combustion conditions. Although the transition probability for BeO(g) emission is low relative to that of BO_2(g), the concentration of the BeO(g) should be sufficiently high as to allow detection. The lack of specific BeO emission may indicate that a

mixed oxide or complex compound is formed. Since thermochemical data relating to these compounds is not available at high temperatures, the usual calculation of theoretical specific impulse includes only BeO and B_2O_3. If, however, a mixed boroberyllium oxide or hydroxide were formed in a metastable or stable state, then the concentration of BeO would be correspondingly reduced. A typical compound of this type is a complex with a structure similar to

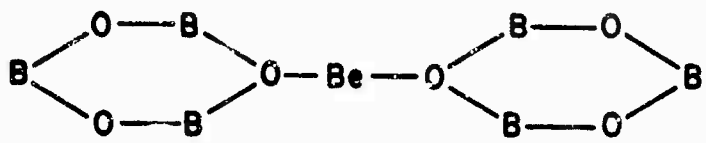

These compounds have been well documented at lower temperatures and would tend to tie up the beryllium and boron in a fully coordinated complex structure. The thermochemical heat release for such compounds would be expected to be somewhat lower than for the formation of a mixture of pure oxides. This would tend to reduce the experimental specific impulse and account, in part, for the observed reduced propellant efficiency.

4. Comments Concerning Observed Spectra

The BO_2 "fluctuation" bands belong to two systems. Each system must involve the ground state since they have been observed in absorption. The spectral assignment made by Johns [illegible]s 4075 Å to the $B^2\Sigma + \rightarrow X^2\pi$ transition and the others to the $A^2\pi \rightarrow X^2\pi$ systems. Of these, the 4075 Å band, although relatively weak in our studies with hybaline, had several resolvable lines where sufficient exposure was available. In the case of the $B^2\Sigma + \rightarrow X^2\pi$ transition the intensity is not sufficient for a rapid scan technique but it may be possible to obtain complementary temperature information in consecutive runs. In any case, the relative intensities of the $B^2\Sigma +$ and $A^2\pi$ systems is of definite interest in analyzing the reaction kinetics involving the BO_2 molecule.

A number of investigators have tried to determine which boron species are responsible for these bands. Before 1961 these maxima had not been completely resolved and were believed to be associated with "continuous emission" from boron, boric acid, or the gaseous B_2O_3. Kaskan and Millikan (4), from a quantitative study of the absorptivity of boron flames at 5740 Å together with data concerning the OH

concentration and emissivity at 2040 Kaysers (HBO_2), suggested that the most likely emitter is BO_2. In more recent studies Kaskan and Millikan (5, 6), and others (2, 7, 8) have confirmed the assignment of these bands to the $BO_2(g)$ species. The best evidence for this assignment has involved high temperature furnace (B_2O_3-O_2) and flash photolysis studies. From the flash photolysis studies involving a BCl_3-O_2 system, Johns (2) was able to obtain low temperature absorption bands which corresponded to those previously seen in emission. Sufficient resolution was available for an analysis of these bands and they were assigned to a linear and symmetric triatomic molecule AB_2 containing only one boron atom. Because of nuclear spin considerations this assignment was made to BO_2 and not BCl_2.

One of the most important implications of the above studies is that the BO_2 fluctuation band does not arise from transitions between two electronic energy levels one of which is unstable. The result of such an instability would be a nonprecise definition of transition energy resulting in continuum band radiation. The work of Johns, in particular, would indicate that these bands are generated via transitions between stable states. The reason that this fact is important to the present studies is that it implies that the states responsible for emission of the BO_2 "fluctuation" bands are in chemical equilibrium with other BO_2 electronic states. Using the principle of detailed balancing it is then possible to relate spectral intensity data to the relative populational distributions of BO_2 at specific electronic energy levels and these distribution functions can then be used to provide species concentration levels. On the other hand, if an unstable state were responsible for the emission then the use of normal statistical methods to obtain concentration data might not necessarily be valid, and the problem of interpreting relative spectral data from boron fueled rocket plumes would be much more complicated.

The OH bands have been reported by a number of investigators and can be seen in Figures 16 and 17, which are typical of spectra obtained from a Hybaline B-3 augmented hydrogen-oxygen flame. These bands are attributed, at least in part, to a chemiluminescent reaction. Although the kinetic path has not been fully worked out, a considerable technical effort has been made to determine the reaction sequence and probable precursor species responsible for the observed chemiluminescence. These reactions may involve either a bimolecular or

trimolecular reaction mechanism to produce the observed species. At ambient pressure the rate constant for the reaction

$$H + OH + OH \rightarrow H_2O + OH^*$$

was measured and found to be $2 \times 10^{-32} cm^6 sec^{-1}$.

This trimolecular reaction has been suggested by several investigators (1, 9) as being responsible for the observed OH chemiluminescence. Based on this reaction rate, an estimate can be made of the relative concentrations of OH* formed by this three body collision process and the thermalysis of the OH radicals by collisional activational processes.

An analysis of this type shows that the concentration levels of OH* are pressure and temperature dependent functions involving two almost independent mechanisms. It is therefore necessary to have sufficient information regarding the relative effects of thermal and chemical activation mechanisms before correlations between the observed intensity levels and the calculated [OH] radical concentration levels can be made with high analytical precision.

III. DISCUSSION

A. General

The major objective of this research program was to determine the feasibility of using emission spectra to analyze high temperature combustion species in rocket exhausts. Such an analysis can provide a "real time" evaluation of the gaseous components in a rocket exhaust stream without perturbing the system in any way by a sampling procedure. The detailed quantitative analysis of emission spectra is exceedingly complicated, both experimentally and analytically. To more closely define the experimental variables, the general technical approach was to use a burner in which Hybaline B-3 was injected into preselected flames simulating rocket exhaust plumes. Emission spectra obtained from such Hybaline B-3 fueled flames were then analyzed. The results of this work indicate that a determination of several specific combustion species can be performed (at least qualitatively) using emission spectroscopy. These species are: $BO_2(g)$, $OH(g)$, $CO_2(g)$, $CO(g)$, $H_2O(g)$, $HBO_2(g)$ and $BO(g)$.

Because of the complexity of the emission spectra in all of the flame systems studied, a considerable effort was necessarily devoted to correlating the observed spectral lines with specific combustion species. A number of difficulties exist in such correlations. They are caused primarily by two effects; first, by the overlapping of spectral bands and lines in a given region by two or more species, and second, by the existence of a broad band continuous emission caused by the continuum of "grey body" radiation eminating from solid or liquid products of reaction. To identify important species a preliminary series of experiments were performed to outline the emission characteristics under conditions which involved relatively simple emission profiles. These were then used to calibrate the spectrographs and to provide a reference base for further investigation.

There is a question as to whether or not a quantitative determination of the absolute concentration levels of individual species can be obtained using emission spectroscopy if a high level of accuracy is required. However, it is probable that a method to determine species concentration levels can be developed using the relative intensity ratios. Such a method would require the use of correlation parameters which are functions of the following: (1) temperature, (2) estimated background interference, (3) relative band overlapping, and (4) optical depth

of the flame zone. Such an analysis would be useful in determining the relative changes in species concentrations which would give an insight into the reaction kinetics.

The sensitivity and precision of such analyses is expected to be a function of the specific combustion product. For example, a strong emission in the 5.5-6.0 micron spectral region has been tentatively identified with the $HBO_2(g)$. This band is extremely intense (indicating probable chemiluminescence) and may possibly be useful in tracing the presence or absence of equilibrium involving the following reaction:

$$H_2O + B_2O_3(c) \rightleftharpoons HBO_2(g).$$

A similar effect was observed for hydroxyl radical emission in the ultraviolet region. For both species the intensity of emission is sufficiently high to allow the use of empirical correlation parameters.

A secondary objective of this program was to determine whether or not the solids produced in the combustion of metalized fuels are completely oxidized. We would thus know if the products corresponded to those which are assumed for theoretical, shifting equilibrium calculations of specific impulse. Therefore, in addition to determining the feasibility of using emission spectroscopy to examine rocket exhaust combustion products, a portion of this work effort was devoted to the chemical analysis of the condensate particles obtained from Hybaline B-3 fueled flames. The results of these chemical analyses indicate the existence of a significant amount of hydrolyzation of the beryllium and boron oxides, particularly at the lower temperatures. From these analyses it is inferred that the early pyrolysis of Hybaline B-3 probably results in the evolution of hydrogen which burns to form water. This implies that the actual oxidation mechanism of the residual boron and beryllium may occur via an oxidation involving water as the oxidizer. If this in fact is the reaction path, then the lack of efficiency of Hybaline B-3 fuels may be attributed to a partial retention of some water vapor in the form of chemically bound water of hydration. This would result in the preferential formation of nonequilibrium products of reaction, and therefore, reduced propulsion efficiency. A more complete discussion of these effects is given in the following sections.

B. Emission Spectroscopy Theory

The observed emission of rocket exhaust plumes is dependent on the species concentration, plume temperatures, and plume thickness. Spectroscopic intensities obtained in emission usually result from a combination of emission and self-absorption. Either photographic plates or an electron photomultiplier detector can be used to measure these intensities. The interpretation of intensity data requires information in addition to the measured intensity determination. The intensity of a given spectrum line is determined both by its transition probability for emission as well as the extent of reabsorption. The intensity I_0 of a given line measured under conditions of negligible self-absorption is proportional to the number N_e of emitting atoms, the frequency ν, and, the transition probability A_c of the line, thus

$$I_0 \propto \nu A_c N_e .$$

Any quantitative analytical procedure using spectral emission from rocket plumes is based on the existence of a definite relationship between the number of molecules or atoms present and the intensity of the specific radiation. This functional relationship may be expressed as

$$I = f\,(N).$$

For a volume of emitting gas containing N_i molecules, in an excited state E_i above the ground state, a number of these, dN_{ij}, will undergo spontaneous transitions to a lower state, E_j, in a given unit of time. The number dN_{ij} is proportional to the population density N_i and therefore;

$$dN_{ij} = A_{ij} N_i d\tau$$

where, A_{ij} is the Einstein transition probability for spontaneous emission. The emission intensity I_{em} of the spectral line is the energy $h\nu$ emitted per unit time

$$I_{em} = h\nu \frac{dN_{ij}}{d\tau}$$

$$= h\nu A_{ij} N_i .$$

Since photons are emitted isotropically in all directions, only the fraction corresponding to the solid angle $d\Omega/4\pi$ are observed by the detector.

It is useful to rewrite the previous emission expression in terms of oscillator strengths. The expression used to determine the transition probability function, A_{ij}, in terms of oscillator strengths f_{ij} is

$$A_{ij} = \frac{8\pi^2}{\lambda^2} \frac{e^2}{mc} f_{ij},$$

where λ is the wavelength corresponding to the transition $i \rightarrow j$, and e and m are the electron charge and mass. Using this equation, the emitted intensity becomes

$$I_{em} = \frac{8\pi^2 e^2 h}{m\lambda^3} N_i f_{ij}.$$

Since oscillator strengths are tabulated in the literature, this latter expression is more useful.

The observed spectral line intensities result from a combination of emission and self absorption. For rocket plume studies where the optical path is long, the self-absorption can become quite important. It can be shown that the observed intensity can be given by an expression which is proportional to the emission intensity and the optical path length as

$$I = \alpha I_{em} \ell ,$$

where α is a proportionality constant, and ℓ is the optical path length in the absorbing media. If g_i refers to the statistical weight of the i th state, and c is the velocity of light, we have

$$I = \alpha \left(\frac{8\pi hc}{\lambda^3}\right)\left(\frac{N_i}{N_0}\right)\left(\frac{g_0}{g_i}\right) \left[1 - \exp\left(\frac{\pi e^2}{mc} N_0 f \ell\right)\right] .$$

For small values of ℓ this expression reduces to

$$I = \alpha \ell I_{em} = \alpha \left(\frac{8\pi^2 e^2 h}{m\lambda^3}\right)\left(\frac{N_i}{N_0}\right)\left(\frac{g_0}{g_i}\right) (N_0 f \ell)$$

which is the same as that previously obtained. This expression allows the analyses of plume thickness effects by using selected changes in specie concentrations obtained from carefully controlled burner studies.

C. Experimental Example

In order to provide quantitative data concerning the relative specie concentrations, it is necessary to correlate the observed spectral intensities with those predicted from a knowledge of the gas compositions and transition probability functions. The observed intensity is a combination of thermal and chemical activation processes which promote the molecules into higher excited states. In most cases the excitation is thermal in origin and therefore the concentrations are directly related to the intensities providing the transition probability function is known. Species which were studied in this research program for which chemical activation is important are OH, CO_2, and HBO_2 (?). For chemiluminescence the spectral intensities will depend on the specific reaction rates responsible for the production of the excited state which may or may not be pressure dependent. Further, even though the specific rate constant and the reaction may be known, there may be an undetermined effect caused by the fall off of the kinetic rate constant at the pressure normally encountered in rocket chambers.

An example case which suffices to illustrate the feasibility of using emission spectra to qualitatively determine rocket exhaust plume concentration gradients is given by a series of three tests performed on this research program. A series of burner runs were made in which Hybaline B-3 was added to hydrogen-oxygen flames corresponding to a variation in O/F mixture ratios. Spectral plates obtained are reproduced in Figure 16. Theoretical calculations predicting the relative concentrations under adiabatic flame conditions are given in Tables II, III, and IV. These calculations correspond to three specific test runs. The species which were prominent in the visible and ultraviolet spectral regions are $BO_2(g)$ and OH(g). The relative equilibrium ratios of OH/BO_2 vary between 0.68 and 1.30 for this series of tests.

There are two methods by which this data can be used to provide information. One is to examine the variation of "absolute" spectral intensities as a function of changes in O/F mixture ratio and thermochemically calculated concentrations for individual species. To properly perform this, the actual flame temperature should be measured. This can be done either by optical pyrometric methods, or by a study of the relative line intensities available from a vibrational analysis of one or more species. The second approach is to correlate the ratios of corrected observed band intensities. A calculation using a ratio of intensities essentially assumes that within a given temperature range

TABLE II. THEORETICAL THERMODYNAMIC COMBUSTION PROPERTIES OF HYBALINE B-3

		Chemical Formula	Wt. Fraction (See Note)	Enthalpy Cal/Mol	State	Temp Deg. K	Density G/CC
Fuel	H 2		0.22000	0.000	G	298.16	0.000000
Fuel	H 13	CNB_2Be	0.78000	-8400.000	L	298.16	0.650000
Oxidant	O 2		1.00000	0.000	G	298.16	0.000000

O/F = 2.470000, Percent Fuel = 28.8184, Equivalence Ratio = 1.6120

EQUILIBRIUM THERMODYNAMIC PROPERTIES

P, ATM	0.8320	0.0011	40.00
T, DEG K	3051	2358	3561
H, CAL/G	-27.1	-27.1	-27.1
S, CAL/(G) (K)	4.4456	5.3920	3.9292
M, MOL WT	14.527	13.504	15.306
CP, CAL/(G) (K)	3.8415	9.0744	2.0855
GAMMA	1.1179	1.0887	1.1396

MOLE FRACTIONS

BO(g)	0.00158	0.00051	0.00204
BO_2(g)	0.05346	0.06444	0.03897
B_2O_2(g)	0.00001	0.00000	0.00007
B_2O_3(g)	0.00063	0.00011	0.00172
Be(g)	0.00056	0.00030	0.00026
BeH(g)	0.00001	0.00000	0.00003
BeO(g)	0.00024	0.00008	0.00015
BeO_2H_2(g)	0.00024	0.00004	0.00043
Be_2O_2(g)	0.00155	0.00056	0.00065
Be_3O_3(g)	0.00148	0.00119	0.00028
Be_4O_4(g)	0.00015	0.00007	0.00003
CO(g)	0.04031	0.03624	0.04236
CO_2(g)	0.00481	0.00567	0.00474
H(g)	0.11522	0.20765	0.06269
H_2(g)	0.34033	0.29061	0.36268
HBO_2(g)	0.03392	0.01866	0.04965
H_3BO_3(g)	0.00000	0.00000	0.00004
HCO(g)	0.00000	0.00000	0.00003
H_2O(g)	0.30055	0.26118	0.33307
N(g)	0.00000	0.00000	0.00001
N_2(g)	0.02207	0.02071	0.02304
NH(g)	0.00000	0.00000	0.00001
NH_3(g)	0.00000	0.00000	0.00001
NO(g)	0.00099	0.00050	0.00103
O(g)	0.00733	0.01572	0.00279
O_2(g)	0.00259	0.00592	0.00100
OH(g)	0.03609	0.03334	0.02819
BeO(s)	0.00000	0.03650	0.00000
BeO(l)	0.03586	0.00000	0.04402

Additional products which were considered but whose mole fractions were less than 0.00005 for all assigned conditions.

B(g)	B_2(g)	BH(g)	BH_3(g)	BN(g)	C(g)	C_2(g)
CH_2(g)	CH_3(g)	CH_4(g)	C_2H_2(g)	C_2H_4(g)	CN(g)	C_2N_2(g)
NO_2(g)	N_2O(g)	N_2O_4(g)	C(s)	Be(s)	Be(l)	B_2O_3(s)
B(s)	B(l)					

C_3(g)	CH(g)
$H_{3B3}O_6$(g)	HCN(g)
B_2O_3(l)	BN(s)

TABLE III. THEORETICAL THERMODYNAMIC COMBUSTION PROPERTIES OF HYBALINE B-3

		Chemical Formula	Wt. Fraction (See Note)	Enthalpy Cal/Mol	State	Temp Deg. K	Density G/CC
Fuel	H 2		0.17000	0.000	G	298.16	0.000000
Fuel	H 13	CNB,Be	0.83000	-8400.000	L	298.16	0.650000
Oxidant	O 2		1.00000	0.000	G	298.16	0.000000

O/F = 2.610000, Percent Fuel = 27.7008, Equivalence Ratio = 1.4284

EQUILIBRIUM THERMODYNAMIC PROPERTIES

P, ATM	0.8320	0.0011	40.00
T, DEG K	3113	2385	3676
H, CAL/G	-27.7	-27.7	-27.7
S, CAL/(G) (K)	4.1462	5.0095	3.6775
M, MOL WT	15.962	14.774	16.922
CP, CAL/(G) (K)	4.1981	9.8148	2.2706
GAMMA	1.1145	1.0865	1.1341

MOLE FRACTIONS

BO(g)	0.00173	0.00052	0.00238
BO_2(g)	0.06646	0.07553	0.05284
B_2O_2(g)	0.00001	0.00000	0.00005
B_2O_3(g)	0.00057	0.00010	0.00161
Be(g)	0.00068	0.00036	0.00035
BeH(g)	0.00001	0.00000	0.00003
BeO(g)	0.00039	0.00011	0.00029
BeO_2H_2(g)	0.00027	0.00004	0.00049
Be_2O_2(g)	0.00241	0.00086	0.00111
Be_3O_3(g)	0.00203	0.00176	0.00042
Be_4O_4(g)	0.00020	0.00011	0.00004
CO(g)	0.04408	0.03937	0.04638
CO_2(g)	0.00654	0.00742	0.00665
H(g)	0.12396	0.21451	0.07150
H_2(g)	0.27623	0.23753	0.29069
HBO_2(g)	0.03192	0.01733	0.04755
H_3BO_3(g)	0.00000	0.00000	0.00004
HCO(g)	0.00000	0.00000	0.00003
H_2O(g)	0.30780	0.26059	0.34808
N(g)	0.00000	0.00000	0.00001
N_2(g)	0.02446	0.02300	0.02550
NH(g)	0.00000	0.00000	0.00002
NO(g)	0.00169	0.00079	0.00203
O(g)	0.01370	0.02584	0.00623
O_2(g)	0.00609	0.01184	0.00291
OH(g)	0.05123	0.04355	0.04449
BeO(s)	0.00000	0.03883	0.00000
BeO(l)	0.03818	0.00000	0.04827

Additional products which were considered but whose mole fractions were less than 0.000005 for all assigned conditions.

B(g)	B_2(g)	BH(g)	BH_3(g)	BN(g)	C(g)	C_2(g)
CH_2(g)	CH_3(g)	CH_4(g)	C_2H_2(g)	C_2H_4(g)	CN(g)	C_2N_2(g)
NH_3(g)	NO_2(g)	N_2O(g)	N_2O_4(g)	C(s)	Be(s)	Be(l)
BN(s)	B(s)	B(l)				

C_3(g)	CH(g)
$H_3B_3O_6$(g)	HCN(g)
B_2O_3(s)	B_2O_3(l)

TABLE IV. THEORETICAL THERMODYNAMIC COMBUSTION PROPERTIES OF HYBALINE B-3

		Chemical Formula	Wt. Fraction (See Note)	Enthalpy Cal/Mol	State	Temp Deg. K	Density G/CC
Fuel	H 2		0.07000	0.000	G	298.16	0.000000
Fuel	H 13	CNB_2F_6	0.93000	-8400.000	L	298.16	0.050000
Oxidant	O 2		1.00000	0.000	G	298.16	0.000000

O/F = 8.930000, Percent Fuel = 10.0705, Equivalence Ratio = 0.3607

EQUILIBRIUM THERMODYNAMIC PROPERTIES

P, ATM	0.8320	0.0011	40.00
T, DEG K	2844	2291	3175
H, CAL/G	-11.3	-11.3	-11.3
S, CAL/(G)(K)	2.6232	3.1187	2.3479
M, MOL WT	27.499	25.981	28.383
CP, CAL/(G)(K)	1.4365	3.5674	0.8466
GAMMA	1.1174	1.0874	1.1408

MOLE FRACTIONS

BO(g)	0.00005	0.00003	0.00003
BO_2(g)	0.05831	0.06083	0.05261
B_2O_3(g)	0.00009	0.00001	0.00026
Be(g)	0.00000	0.00001	0.00000
BeO(g)	0.00004	0.00003	0.00001
BeO_2H_2(g)	0.00017	0.00003	0.00026
Be_2O_2(g)	0.00033	0.00020	0.00008
Be_3O_3(g)	0.00045	0.00045	0.00006
Be_4O_4(g)	0.00005	0.00003	0.00001
CO(g)	0.00818	0.01152	0.00448
CO_2(g)	0.02750	0.02224	0.03225
H(g)	0.01084	0.04021	0.00292
H_2(g)	0.01123	0.02128	0.00521
HBO_2(g)	0.01283	0.00663	0.02026
B_3BO_3(g)	0.00000	0.00000	0.00003
H_2O(g)	0.26349	0.22754	0.28614
N_2(g)	0.01397	0.01533	0.01271
NO(g)	0.00774	0.00311	0.01125
NO_2(g)	0.00001	0.00000	0.00005
O(g)	0.04526	0.08876	0.02070
O_2(g)	0.42987	0.39965	0.45236
OH(g)	0.07633	0.07028	0.06224
BeO(s)	0.00000	0.03185	0.00000
BeO(l)	0.03326	0.00000	0.03610

Additional products which were considered but whose mole fractions were less than 0.000005 for all assigned conditions.

B(g)	B_2(g)	BH(g)	BH_3(g)	BN(g)	B_2C_2(g)	BeH(g)
C_2(g)	CH(g)	CH_2(g)	CH_3(g)	CH_4(g)	C_2H_2(g)	C_2H_4(g)
$H_3B_3O_6$(g)	HCN(g)	HCO(g)	N(g)	NH(g)	NH_3(g)	N_2O(g)
Be(s)	Be(l)	B_2O_3(s)	B_2O_3(l)	BN(s)	B(s)	B(l)
C(g)	C_3(g)					
CN(g)	C_3N_2(g)					
N_2O_4(g)	C(s)					

the parameters affecting the specific emission intensities are similar for each species. This method has the advantage of being related more closely to changes in kinetic processes via changes in relative species concentrations.

"Absolute" spectral intensities were obtained for OH(g) and BO_2(g) using spectra taken in the ultraviolet and visible region. The observed film densities were then corrected for a number of experimental and theoretical quantities to provide corrected observed band intensities. The correspondence between the observed band intensities and O/F mixture ratio is given in Figures 20 and 21 for OH(g) and BO_2(g), respectively. Because of the general continuum background which extends through much of the visible region, the lower BO_2(g) fluctuation bands were used in order to reduce the experimental uncertainty.

As can be seen, there is a reasonable correspondence between the observed and calculated values. An estimate of the experimental error is given by the bar line values for the experimental points. Using the ratio method, a plot of observed intensities for three O/F mixture ratios was made for the OH/BO_2 system, Figure 22. In this plot, the theoretically calculated intensity variations are given together with the experimental values. These results show a good correspondence between the predicted and experimental observations. For this system, the predicted ratio of intensities changes by a factor of 2 over the range of study, and the observed intensity ratios at the high and low ends of the O/F ratio curve reflect this difference. For the purpose of a qualitative description of concentration changes, these results indicate that emission spectroscopy can be used to provide useful information. With more precise optical measurements, it may be possible to provide significant kinetic rate data for intermediate species.

These results indicate the feasibility of using changes in spectral emission characteristics of rocket plumes for at least qualitative analysis of the exhaust products in "real time." A similar comparison can be made using data obtained in the infrared region, but because simultaneous observation could not be easily performed with present instrumentation, correlations between BO_2(g) and H_2O, BO_2(g) and CO_2, and BO_2(g) and HBO_2 were not made on this program. It is believed that from careful analysis using a band and line summation method, quantitative data may be obtained. One of the more interesting possibilities is using the 5.5 - 6.0 micron emission band of HBO_2(g) together

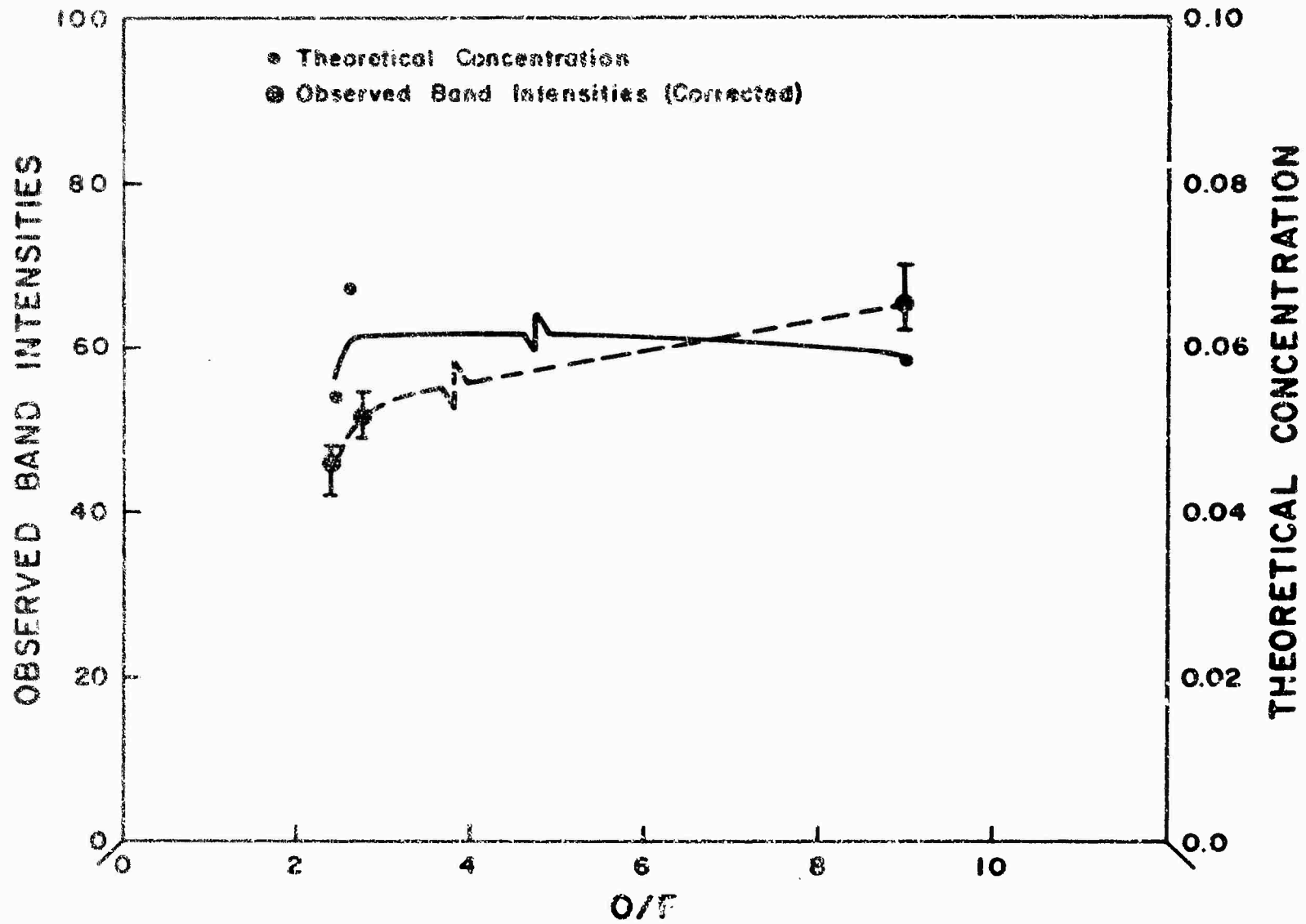

Figure 20. Correlation of Band Intensity with O/F and Calculated Concentrations of Hydroxyl Radical

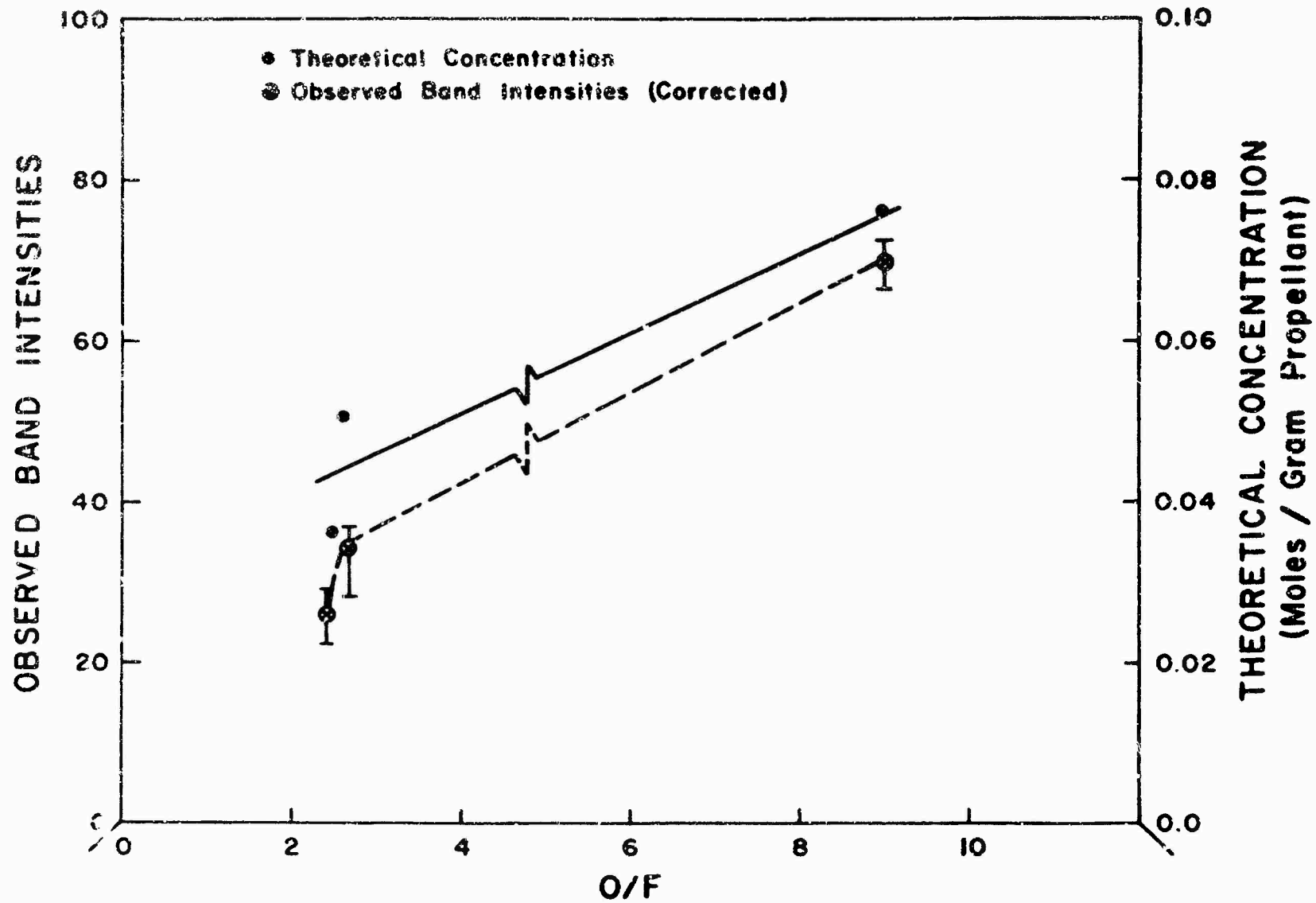

Figure 21. Correlation of Band Intensity with O/F and Calculated Concentrations of $BO_2(g)$

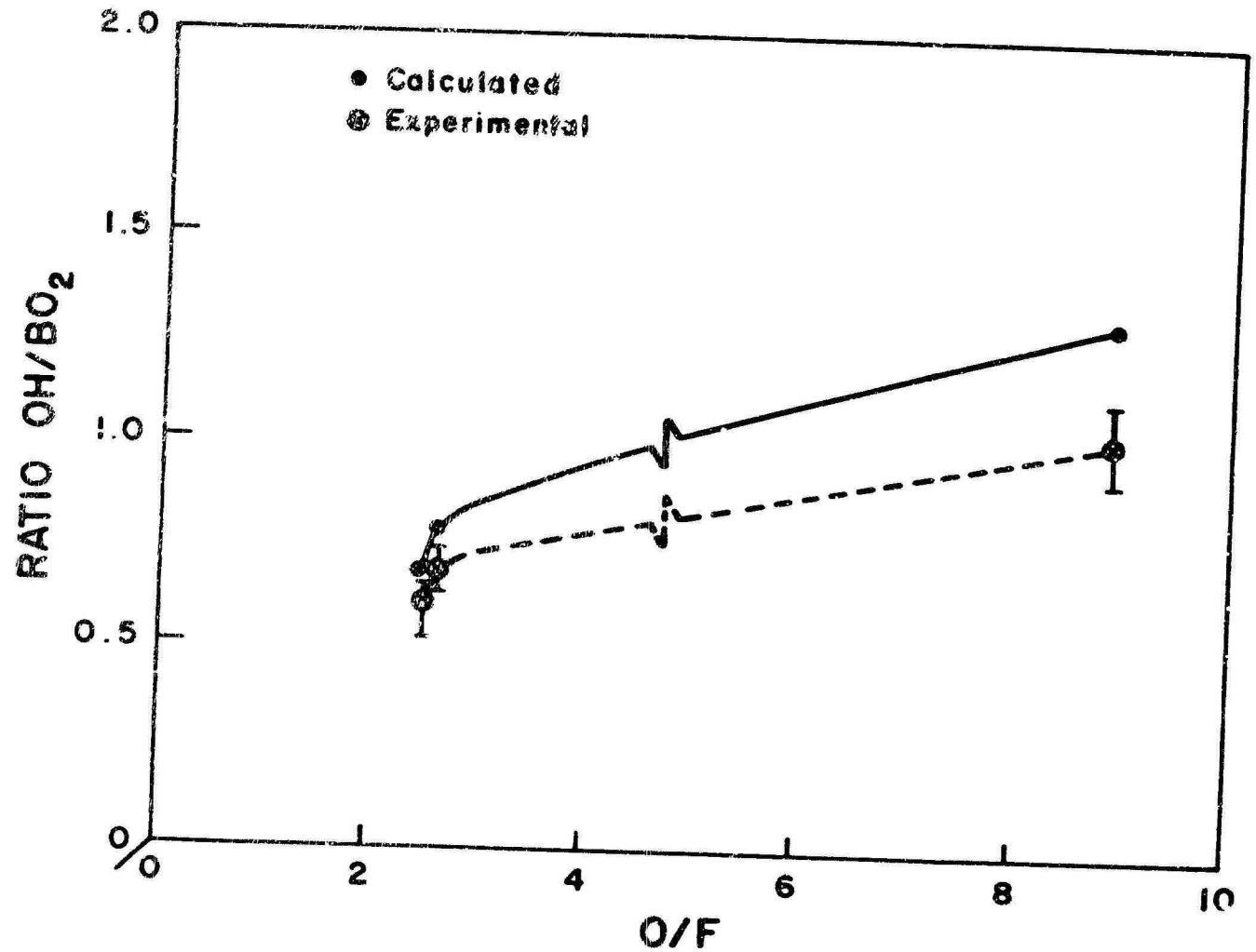

Figure 22. Correlation Between Calculated Species Concentrations and Observed Relative Spectral Emission for the Ratio OH/BO_2

with the $BO_2(g)$ fluctuation bands to follow the extent of $HBO_2(g)$ formation under conditions of fuel-rich combustion. This would have specific application to air-augmented boron-fueled ramjets.

D. Combustion Model

The combustion efficiency of Hybaline B-3 fueled rockets is considerably below that observed for other rocket propellant systems. Therefore, one of the purposes of this program was to attempt to find methods suitable for determining the species concentrations at selected combustion environmental conditions. To do this, a preliminary attempt was made to formulate a model capable of describing the physical and chemical factors important to the pyrolysis and combustion of Hybaline B-3 fueled propellant systems. At the present time this model is quite speculative, being based on fragmentary evidence obtained on this program together with observations from other laboratories.

In brief, it is proposed that the pyrolysis of the atomized fuel is the first rate limiting step. It is probable that the pyrolysis of Hybaline B-3 proceeds through a thermal decomposition to form diborane, since this decomposition has been observed to occur in the storage and thermalization of Hybaline B-3. Because the temperature in the immediate region of the droplet cannot substantially exceed that of the liquid droplet, it would be expected that low temperature reaction products would be formed. A second step would involve the thermal decomposition of diborane to form B(c) and hydrogen gas. Because the diffusion rate of the hydrogen is relatively rapid, it would be expected that the combustion zone located at some distance from the droplet surface would effectively consist of a hydrogen-oxygen reaction producing water. In this model in the steady state, the oxidation of the metals boron and beryllium would tend to take place by a high temperature hydrolysis reaction rather than by a direct oxidation. Conditions like these would provide relatively high concentrations of hydrogen and boron, and thus tend to favor the production of polymeric boron oxides possibly linked together by beryllium bridging structures. These conditions would be close to those used for high temperature mass spectral equilibrium studies by Sholette and Porter (23). These postulations would also explain the possible production of a hydrated polymeric structure capable of emitting at wavelengths past 4.5 microns in the infrared region.

A comment is in order concerning the types of polymeric structures of boron oxide expected from these reaction conditions. The

thermal stability of the trimer $(HBO)_3$ is relatively high providing the concentration of oxygen is above a critical minimum value. However, for a droplet burning mechanism in which the initial pyrolysis produces hydrogen and boron more or less directly, the formation of boroxine would be expected rather than the more highly oxidized species. From a chemical structures point of view, this trimer $H_3B_3O_3$ is but one of a number of possible reaction products, the others including primarily the hydroxyboroxines and their polymers. Thus, for fuel rich environments such as those surrounding the droplet, the production of boroxines and derivatives thereof would be predicted. Because of the increased thermochemical stability of B_2O_2 and HBO_2, the production of these latter compounds would be expected to occur as an afterburning in an oxidizing atmosphere. Since boroxine possesses considerable kinetic metastability, it would be expected a high activation energy would be required to produce the thermochemically calculated equilibrium distribution of reaction products. Therefore, its existence could possibly account for many of the observed kinetic losses present. A polymerized form of boroxine involving a beryllium linkage would be expected to occur as a reaction intermediate.

The infrared absorption spectrum of boroxine has been investigated by Wason and Porter (22), and is presented in Table V.

TABLE V. INFRARED SPECTRUM OF BOROXINES

Boroxine		Deuterated Boroxine	
Frequency (cm^{-1})	Intensity	Frequency (cm^{-1})	Intensity
2620	S.	1948	S.
1394	V.S.	1378	V.S.
1384	V.S.	1368	V.S.
1213	m.	--	--
937	m.	--	--
918	s.	811	S.

Partial Vibrational Assignment

2620	1948	Assymetric B-H stretch
1389	1373	Ring stretch
1213	--	Ring stretch
918	811	Out of plane B-H bend

No data were available on the emission spectra in either the infrared or visible regions for boroxine, and the reaction precursors of the boroxine derivatives are not known. However, estimates of the infrared emission band locations and their relative strengths can be made using the above table. The expected major spectral emission bands are estimated to be at about 3.8 and 7.2 microns. Since the instrumental infrared cut-off point for these studies was about 6.3 - 6.5 microns, the 7.2 micron bands could not be observed directly. Examination of the spectrum presented in Figure 6 shows a weak emission band in the 3.8μ region. Because of overlap with the 2.7μ peak of CO_2 only a tentative identification is possible. Although the expected band is relatively strong, the emissivity may be low because of relatively low overall concentration levels. If this peak is related to the existence of a metastable boroxine molecule, there would be two degradation effects on specific impulse. The specific impulse would be reduced because of reduced thermochemical energy and because of an increase in the average molecular weight of the propellant gas stream.

It is becoming more apparent that the fundamental chemistry of the precursor and metastable species is not understood, and that important parts of the infrared emission spectrum from Hybaline B-3 fueled flames may result from emissions from these intermediate species. Additional experimental studies involving Hybaline B-3 augmented, deuterium-oxygen flames are suggested for the future to determine whether the expected strong shift from deuterium substituted boroxines can be observed.

E. Intermediate Pyrolysis Products

One of the observations which has been made during the course of Hybaline B-3 flame studies is that there is a soot produced in most cooler flames. These particles consist of light-weight brownish white solid combustion products. They are produced in the lower flame regions and traverse more or less unmodified through the hotter combustion zones. The interest in these particles stems from the fact that they may represent an intermediate reaction species through which the Hybaline B-3 must pass before reaching thermochemical equilibrium conditions. A knowledge of these intermediate species is important in outlining the chemical mechanisms governing the combustion inefficiencies in rocket propellants containing boron and beryllium compounds.

An analysis of the chemical composition of these particles was attempted in order to determine the structure of these soots. The results of these analyses are inconclusive, although some tentative and speculative conclusions can be reached.

Two samples of "soot" formed in a Hybaline B-3 - air diffusion flame were subjected to X-ray analysis to determine chemical structure. One sample was taken from a residue obtained from the slow air oxidation of Hybaline B-3. This sample had no detectable line structure, indicating a fully amorphous material. The second sample was taken from the upper region of the flame zone. This material had limited line structure, but no positive identification could be made with the known oxides, nitrides, or carbides, of either boron or beryllium. The indications are that an ordered but largely amorphous material is present.

A second series of samples was submitted to Coors Analytical Laboratory for analysis using arc spectrographic and wet chemical methods of analysis. The results of these analyses are presented in Table VI for three different types of samples.

TABLE VI. COMPOSITION OF SOOT FORMED IN COMBUSTION OF HYBALINE B-3

	A "Soot"		B Slow Air	C Ash
	Arc Spectra	Wet Chemical	Reaction Arc Spectra	Residue Wet Chemical
Beryllium	2%	4%	1%	20.0%
Boron	2%	9.36%	5%	14.3%
Carbon	7.8%	---	9.35%	---
Nitrogen	---	---	0.005%	---

Sample A was "soot" obtained from a location about six inches above the top surface of the flame. This sample consists of fluffy particles which originate below the actual combustion zone and which traverse the high temperature regions. Sample C consisted of the residue ash obtained from an injector head dispersing the liquid Hybaline B-3 into a high temperature hydrogen-oxygen flame Sample B was obtained from the residue formed by Hybaline B-3 upon air contact at room

temperature. It is apparent from a comparison of the values obtained by the two analysis methods used on the soot that there is some inconsistency in the results. This inconsistency is probably due to the fact that the arc spectrographic techniques are usually used for trace amounts rather than concentrations in the one percent or greater range. However, this method should be able to provide valid results for concentrations up to four percent.

Assuming that the wet chemical method provides reasonably correct analytical results, it is useful to estimate the composition of the mixture. For this purpose it is also assumed that the carbon content as determined spectroscopically is correct since a carbon analysis was not performed for the wet chemical analyses. If a fully oxidized metal content is assumed, i.e., the sample is a mixture of beryllium oxide and boron oxides, then the maximum oxide weight attributable to the beryllium and boron is 6.6 and 20.5 percent, respectively. However, this yields a total sample weight of only 48 percent of the sample submitted. A possible gain of a few percent could be obtained by allowing some carbonate formation but no major change can be made in the conclusion that roughly fifty percent of the sample is unaccounted. From the spectroscopic analysis it is certain that no significant amounts of other metals are present, a result which would be expected from the chemical composition of the fuel and oxidizer. While the precision of analysis is somewhat questionable, it is very improbable that the reported wet chemical results are in error by more than ten to twenty percent.

The tentative conclusion indicated by these results is that the remainder of the sample must be composed largely of water. Boron forms a great variety of stable hydrates which would be expected to condense under the lower temperature conditions in the air diffusion flame. The most likely prospect is that a molecule such as metaboric acid could be formed from the polymerization of HBO_2 to form a basic trimeric structure. In this quite speculative view, a hyba'ne droplet would oxidize to form a flexible exterior oxide-hydroxide sheath. The combustion reaction would require both the diffusion of hydrogen formed by a pyrolytic decomposition of diborane in the interior section of the droplet, and the counterdiffusion of oxygen from the exterior section of the droplet. A reaction to form water would therefore occur in close proximity to a solid hygroscopic surface. A mechanism of this type would account for the extent of hydration which implicitly occurs if the

above analytical procedures are reasonably accurate. At higher flame temperatures partial dehydration of the hydrates would be expected.

IV. SUMMARY AND CONCLUSIONS

A. Summary

During this research program analytical and experimental studies were performed in order to develop a "real time" spectrographic method suitable for determining the extent of chemical and thermal equilibrium present in Hybaline B-3 fueled combustion reactions. Such studies are necessary in order to verify that correct thermochemical data have been utilized in shifting and frozen equilibrium, specific impulse calculations. The method which was developed relied on the use of the observed emission spectra eminating from specific gaseous species using Hybaline B-3 fueled burners. The species observed in emission were $BO_2(g)$, $OH(g)$, CO_2, CO, and H_2O. Data were obtained in all three major spectral regions; i.e., the infrared, the visible, and the ultraviolet. A qualitative correlation was made between theoretical predicted values of species concentrations and observed spectral band intensities. Combustion conditions were chosen to simulate those present in a fuel rich environment similar to that of an operating rocket engine. For this purpose it was assumed that normal oxidizers for Hybaline B-3 would be either hydrogen peroxide or nitrogen tetroxide. Because of experimental convenience these studies were performed using a burner operated at ambient pressure.

An analysis of the spectra in each of the regions was used to provide information concerning the presence of a number of specific combustion species. For a number of reasons, only those species which have a high transition probability can be observed in flames and plumes. Therefore, the observable species constitute only a small fraction of the total number of chemical entities present. A major consideration for combustion systems which produce substantial amounts of condensed species such as BeO and B_2O_3 is whether the specific emission associated with an individual specie can be separated from the overall grey body emission from the solid particles. The results of this program indicate that this separation can be accomplished for $BO_2(g)$ in the visible, $OH(g)$ in the ultraviolet, and $HBO_2(?)$ or B_2O_2 in the infrared. However, grey body emission and broad bands limit the precision to which specific band or line spectra may be measured.

B. Conclusions

The spectrographic techniques developed on this program are feasible for determining the "real time" kinetic behavior of Hybaline B-3 fueled rocket combustion gases. The major advantages of this method are (1) that no perturbation of the system is caused by the sampling of the reaction products, and (2) that no subsequent reactions interfere with the analysis. This technique is adaptable to any propellant using beryllium and boron either as slurries on in compounds.

The results of this research program indicate that sufficient specific emission occurs in the infrared, visible, and ultraviolet spectral regions to allow an analysis of the relative concentration of at least four chemical species. These species are $BO_2(g)$, OH, CO_2, and H_2O. HBO_2 may possibly be a fifth specie capable of detection. Observed intensity ratios can be combined with theoretically predicted thermochemical data to aid in the determination of the existence of metastable species, and to follow the kinetic course of high temperature reactions.

The solid products of reaction are not a combination of pure $BeO(s)$ and $B_2O_3(s)$. It is concluded, tentatively, that these solids contain substantial fractions of hydrogen, either in the form of water of hydration or as chemically stable intermediate compounds. Any hydrogen chemically bound in this manner will substantially lower the specific impulse by increasing the average molecular weight of the propellant gases, and by reducing the thermochemical heat of reaction.

REFERENCES

1. Hinck, E. C., Seamans, T. F., Vanpee, M., and Wolfhard, H. G., "The Nature of OH Radiation in Low Pressure Flames," Tenth Symposium on Combustion, 21-32, The Combustion Institute (1965).

2. Johns, J. W. C., "The Absorption Spectrum of BO_2," Can. J. Phys. 39, 1738-1768 (1961).

3. Johns, J. W. C., Can. J. Phys., 39, 1738-1768 (1961).

4. Kaskan, W. E., and Millikan, R. C., "Source of Green Bands from Boron-Containing Flames," J. Chem. Phys. 32, 1273-1274 (1960).

5. Kaskan, W. E., and Millikan, R. C., "Origin of the Green Bands in the Boron Oxygen System," J. Chem. Phys. 34, 570-574 (1961).

6. Kaskan, W. E., and Millikan, R. C., VIIIth Symposium Combustion, Pasadena, 262-275, (1960), Williams and Wilkins Co., Baltimore (1962).

7. Soulen, J. R., and Margrave, J. L., "Vaporization of Boric Oxide and Thermodynamic Data for the Gaseous Molecular B_2O_3, B_2O_2, and BO," J. Am. Chem. Soc., 78, 2911-2912 (1956).

8. Soulen, J. R., Sthapitanonda, P., and Margrave, J. L., Vaporization of Inorganic Substances, B_2O_3, TeO_2, and Mg_3N_2, J. Phys. Chem., 59, 132-136 (1955).

9. Zeegers, P. H. Th., and Alkemade, C. Th. J., "Chemiluminescence of OH Radicals and K Atoms by Radical Recombustion in Flames," Tenth Symposium on Combustion, 33-40, The Combustion Institute (1965).

10. Kottenstette, J. P., Fast Response Optical Pyrometer, ISA Transactions 4, 270-274 (1965).

11. Williams, R. E., and Evans, R. W., (Secret Report), Experimental Investigation of Infrared Radiating Chemical Sources, AFAL-TR-65-180 (1965).

12. Zeleznik, F. J., and Gordon, S., A General IBM 704 or 7090 Computer Program for Computation of Chemical Equilibrium Compositions, Rocket Performance, and Chapman-Jouguet Detonations, NASA TN D-1454 (1962).

13. Gordon, S., and Zeleznik, F. J., A General IBM 704 to 7090 Computer Program for Computation of Chemical Equilibrium Compositions, Rocket Performance, and Chapman-Jouguet Detonations - Supplement I. Assigned Area-Ratio Performance. NASA TN D-1737 (1963).

14. Pearse, R. W. B., and Gaydon, A. G., The Identification of Molecular Spectra, Chapman and Hall, Ltd., London, 1963, (U).

15. Porter, R. F., and Dows, D. A., "Blue Emission from the Vapor of Burning Boron," J. Chem. Phys., 24, p. 1270, 1956, (U).

16. Mulliken, Robert S., "The Isotope Effect in Band Spectra, II. The Spectrum of Boron Monoxide," Phys. Rev., 25, p. 259.

17. White, D., Mann, D., Walsh, P., and Sommer, A., "Infrared Emission Spectra of Gaseous B_2O_3 and B_2O_2," J. Chem. Phys., 32, p. 481, 1960, (U).

18. White, D., Mann, D., Walsh, P., and Sommer, A., "Infrared Emission Spectrum of Gaseous HBO_2," J. Chem. Phys., 32, p. 488, 1960, (U).

19. Gerrard, W., "The Organic Chemistry of Boron," Academic Press, New York, 1961, (U).

20. Forsythe, W. E., "Measurement of Radiant Energy," McGraw-Hill, New York, 1937, (U).

21. Huff, V. N., Gordon, S., and Morrell, V. E., "General Method and Thermodynamic Table for Computation of Equilibrium Composition and Temperature of Chemical Reactions," National Advisory Committee for Aeronautics, Rept. 1037, 1951, (U).

22. Wason, S. K., and Porter, R. F., "Gaseous Borazine: Infrared Spectrum and Structure," J. Phys. Chem., 68, 1443 (1964).

23. Sholette, W. P., and Porter, R. F., "Mass Spectrometric Study of High Temperature Reactions in the Boron-Hydrogen-Oxygen System," J. Phys. Chem. 67, 177 (1963).

PREVIOUS PAGE WAS BLANK, THEREFORE WAS NOT FILMED.

APPENDIX I - MAJOR SPECIES

APPENDIX I - MAJOR SPECIES

APPENDIX IA. SPECTRAL CHARACTERISTICS OF SELECTED MAJOR COMBUSTION PRODUCTS

Species		Visible (Å)			IR (cm^{-1})	
CO		3911	4557	4932	2198	1596
		4154	4577	4981	2170	1576
		4260 max.	4654	5026	2134	1558
		4344	4659	5129	2133	1516
		4413	4769	5169	2112	1326
		4485	4798	5278	2082	1218
		4528	4896	5318	1739	1138
				5430	1620	1097
CO_2					4978	1343
					3715	667
					2349	
H_2O		5692	8227	9378		
	weak	↓	8228	9381		
		8161	8274	9387		
	absorption	8162	8282	9427		
		8165	8288	9428		
		8170	8992	9438		
		8177	9000	9440		
		8189	9344	9460		
		8193	9372	9461	5331	
		8198		9522	3756	gas
				9545	3657	gas
					1595	gas
	emission	4216	7165		3445	
		4337	8097		3219	liquid
		4587	8916		1627	liquid
		4731	9277			
		5126	9333			
		5480	9669			
OH		9500			3735	
					3181	
					2210	
					660	

APPENDIX IA (Continued)

Species	Visible (Å)			IR (cm^{-1})
OH^+				2955
				1986
Be	3455	3865		
	3515	4408		
	3736	4573		
	3813	5908		
Be^+	4674			
BeH	4981 h	4991 Q		2133
	4983 Q	5508 h		2088
	4985 Q	5537 h		2057
	4988 h			
BeH^+	2385-3082			2222
				1476
*BeO	4427	5076	7955	1487
	4452	5095	8206	1371
	4475	5112	8469	1144
	4496	6287	8713	1082
	4708	6344	9003	1016
	4733	6524	9648	
	4755	7325	10300	
	5054	7953	10800	
			11200	
BeOH				bend 1000-970
				3740
				1525
				1276
BeN				1194
				stretch 850-650
BeC_2				1947
				1580
				423
B	(ultraviolet)			

APPENDIX IA (Continued)

Species	Visible (Å)			IR (cm^{-1})	
B^+	3179				
	3451				
BH	3662 R	4332 Q		2400	
	3694 Q	4367 Q		2366	
	4264 R	4434 Q		2344	
	4319 R			2230	
HBO				bend 1000-970	
				2300	
				1900	
				700	
$*HBO_2$				3680	1250
				2030	700
				1420	600
*BO	3388	3849	4586	stretch 2100-900	
	3511	4017	4589		
	3525	4035	4613	1885	
	3527	4037	4615	1280	
α	3662	4143	4744	1261	
	3678	4146	4747		
	3679	4339	5040		
	3828	4342	5548		
	3830	4363	5552		
	3847	4366			
β	2200-3400				
combination	4577-5916 weak				
upper β	5361	5777			
	5395	5781			
	5479	5790			
$*BO_2$	4520	5800		O-B-O stretch 900-600	
	4710	6030			
	4930	6200		2080	570
	5180	6390		2065	565
	5450			1910	435
				1890	285
				610	215

APPENDIX IA (Continued)

Species	Visible (Å)	IR (cm^{-1})	
*B_2O_3		2095	730
		2073	521
		2041	480
		1302	460
		1240	457
		746	172
BN	2900-3250 singlet	1515	
	3400-4000 triplet	1317	
		stretch 850-650	
BC		1350-1300	
BN_{ring} (Borazole)		1473-1373	
Boron - amine complex			
$B_3N_3H_6$?		1100	

APPENDIX IB. COINCIDENCE TABLE FOR SELECTED MAJOR COMBUSTION PRODUCTS IN THE VISIBLE REGION

3451 - B^+
3455 - Be
3511 - BO
3515 - Be
3525 - BO
3527 - BO
3662 - BH, BO
3678 - BO
3679 - BO
3694 - BH
3736 - Be
3813 - Be
3828 - BO
3830 - BO
3847 - BO
3849 - BO
3865 - BO
3911 - CO
} BN

4017 - BO
4035 - BO
4037 - BO
4143 - BO
4146 - BO
4154 - CO
4216 - H_2O_e
4260 - CO
4264 - BH
4319 - BH
4332 - BH
4337 - H_2O_e
4339 - BO
4342 - BO
4344 - CO
4363 - BO
4366 - BO
4367 - BH
4408 - Be
4413 - CO
4427 - BeO
4434 - BH
4452 - BeO
4475 - BeO
4485 - CO
4496 - BeO
4510 - BO_2
4528 - CO
4557 - CO
4573 - Be
4577 - CO
4586 - BO
4587 - H_2O_e
4589 - BO
4613 - BO
4615 - BO
4654 - CO
4659 - CO
4674 - Be^+
4708 - BeO
4710 - BO_2
4731 - H_2O_e
4733 - BeO
4744 - BO
4747 - BO
4755 - BeO
4769 - CO
4798 - CO
4896 - CO
4930 - BO_2
4932 - CO
4981 - BeH
4983 - BeH
4986 - BeH
4988 - BeH
4991 - BeH
5026 - CO
5040 - BO
5054 - BeO
5076 - BeO
5095 - BeO
5112 - BeO
5126 - H_2O_e
5129 - CO
5169 - CO
5180 - BO_2
5278 - CO
5318 - CO
5361 - BO
5395 - BO
5430 - CO
5450 - BO_2
5479 - BO
5480 - H_2O_e
5508 - BeH
5537 - BeH
5548 - BO
5552 - BO
5777 - BO
5781 - BO
5790 - BO
5800 - BO_2
5908 - Be
6030 - BO_2
6200 - BO_2
6287 - BeO
6344 - BeO
6390 - BO_2
6524 - BeO
7165 - H_2O_e
7325 - BeO
7953 - BeO
8097 - H_2O_e
8206 - BeO
8469 - BeO
8713 - BeO
8916 - H_2O_e
9003 - BeO
9277 - H_2O_e
9333 - H_2O_e
9500 - OH
} H_2O_a

9648 - BeO
9669 - H_2O_e
10300 - BeO
10800 - BeO
11200 - BeO

APPENDIX IB (Continued)

INFRARED COINCIDENCE TABLE

cm^{-1}

5331 - $H_2O(g)$
4978 - CO_2
3756 - $H_2O(g)$
3740 - BeOH
3735 - OH
3715 - CO_2
3680 - HBO_2
3657 - $H_2O(g)$
3445 - $H_2O(\ell)$
3219 - $H_2O(\ell)$
3181 - OH
2955 - OH^+
2400 - BH
2366 - BH
2349 - CO_2
2344 - BH
2300 - HBO
2230 - BH
2222 - BeH^+
2210 - OH
2198 - CO
2170 - CO
2134 - CO
2133 - CO, BeN
2112 - CO
2095 - B_2O_3
2088 - BeH
2082 - CO
2080 - B_2O_2
2073 - B_2O_3
2065 - B_2O_2
2057 - BeH
2041 - B_2O_3
2030 - HBO_2

1986 - OH^+
1947 - BeC_2
1910 - B_2O_2
1900 - HBO
1890 - B_2O_2
1885 - BO
1739 - CO
1627 - $H_2O(\ell)$
1620 - CO
1596 - CO
1595 - $H_2O(g)$
1580 - BeC_2
1576 - CO
1558 - CO
1525 - BeOH
1516 - CO
1515 - BN
1487 - BeO
1476 - BeH^+
1420 - HBO_2 } BN ring
1371 - BeO
1343 - CO_2
1326 - CO
1317 - BN
1302 - B_2O_3 } BC
1280 - BO
1276 - BeOH
1261 - BO
1250 - HBO_2
1240 - B_2O_3
1218 - CO
1194 - BN
1144 - BeC
1138 - CO

1100 - $B_3N_3H_6$
1097 - CO
1082 - BeO
1016 - BeO
1000-970 - BeOH, HBO
BeN, BN { 746 - B_2O_3, 730 - B_2O_3, 700 - HBO_2, HBO, 667 - CO_2, 660 - OH } O-B-O
610 - B_2O_2
600 - HBO_2
570 - B_2O_2
565 - B_2O_2
521 - B_2O_3
480 - B_2O_3
460 - B_2O_3
457 - B_2O_3
435 - B_2O_2
423 - BeC_2
285 - B_2O_2
215 - B_2O_2
172 - B_2O_3

APPENDIX IC. MOLECULAR SPECTRUM OF BORON DIOXIDE ($B^{11}O_2$) IN FLAMES

Intensity	Band Head Wavelengths (in Å)	Spectral Term Symbols and Vib. Quantum Numbers Lower	Upper	Energy Levels (in ev) Lower	Upper
		X	B		
6	4051.9	$01^10^2\Sigma^{(+)}$	$01^10^2\Pi_{1\frac{1}{2}}$	0.052	3.111
5	4057.2	$01^10^2\Delta_{2\frac{1}{2}}$	$01^10^2\Pi_{1\frac{1}{2}}$	0.057	3.111
10	4065.5	$00^00^2\Pi_{1\frac{1}{2}}$	$00^00^2\Sigma^+$	0.018	3.048
5	4081.5	$01^10^2\Delta_{1\frac{1}{2}}$	$01^10^2\Pi_{1\frac{1}{2}}$	0.075	3.111
10	4090.6	$00^00^2\Pi_{0\frac{1}{2}}$	$00^00^2\Sigma^+$	0	3.048
		X	A		
5	4162.9	$00^00^2\Pi_{1\frac{1}{2}}$	$02^02^2\Pi_{1\frac{1}{2}}$	0	2.977
4	4168.9	$00^00^2\Pi_{0\frac{1}{2}}$	$02^02^2\Pi_{0\frac{1}{2}}$	0.018	2.991
2	4302.6	$00^00^2\Pi_{1\frac{1}{2}}$	$26^00^2\Pi_{1\frac{1}{2}}$	0	2.881
1	4305.1	$00^00^2\Pi_{0\frac{1}{2}}$	$26^00^2\Pi_{0\frac{1}{2}}$	0.018	2.897
2	4335.0	$01^10^2\Sigma^{(+)}$	$01^12^2\Sigma^{(+)}$	0.052	2.911
2	4335.4				
2	4340.0	$01^10^2\Delta_{2\frac{1}{2}}$	$01^12^2\Delta_{2\frac{1}{2}}$	0.057	2.912
7	4340.5	$00^00^2\Pi_{1\frac{1}{2}}$	$00^02^2\Pi_{1\frac{1}{2}}$	0	2.855
1	4348.1	$01^10^2\Delta_{1\frac{1}{2}}$	$01^12^2\Delta_{1\frac{1}{2}}$	0.075	2.926
7	4349.0	$00^00^2\Pi_{0\frac{1}{2}}$	$00^02^2\Pi_{0\frac{1}{2}}$	0.018	2.868
1	4496.8	$00^00^2\Pi_{1\frac{1}{2}}$	$24^00^2\Pi_{1\frac{1}{2}}$	0	2.756
1	4502.5	$00^00^2\Pi_{0\frac{1}{2}}$	$24^00^2\Pi_{0\frac{1}{2}}$	0.018	2.771
1	1503.0	$00^00^2\Pi_{1\frac{1}{2}}$	$16^00^2\Pi_{1\frac{1}{2}}$	0	2.752
1	4506.1	$00^00^2\Pi_{0\frac{1}{2}}$	$16^00^2\Pi_{0\frac{1}{2}}$	0.018	2.769
1	4685.8	$00^00^2\Pi_{1\frac{1}{2}}$	$22^00^2\Pi_{1\frac{1}{2}}$	0	2.645
2	4694.8	$00^00^2\Pi_{0\frac{1}{2}}$	$22^00^2\Pi_{0\frac{1}{2}}$	0.018	2.658
4	4719.5	$00^00^2\Pi_{1\frac{1}{2}}$	$14^00^2\Pi_{1\frac{1}{2}}$	0	2.626

APPENDIX IC (Continued)

Intensity	Band Head Wavelengths (in Å)	Spectral Term Symbols and Vib. Quantum Numbers Lower	Upper	Energy Levels (in ev) Lower	Upper
		X	A		
3	4727.3	$00^00^2\Pi_{0\frac{1}{2}}$	$14^00^2\Pi_{0\frac{1}{2}}$	0.018	2.640
2	4881.0	$01^10^2\Sigma^{(+)}$	$21^10^2\Sigma^{(+)}$	0.052	2.590
2	4882.1				
2	4891.6	$01^10^2\Delta_{2\frac{1}{2}}$	$21^10^2\Delta_{2\frac{1}{2}}$	0.057	2.590
2	4891.8	$00^00^2\Pi_{1\frac{1}{2}}$	$12^20^2\Pi^{(+)}_{1\frac{1}{2}}$	0	2.534
1	4900.0	$01^10^2\Delta_{1\frac{1}{2}}$	$21^10^2\Delta_{1\frac{1}{2}}$	0.075	2.605
7	4906.9	$00^00^2\Pi_{1\frac{1}{2}}$	$12^00^2\Pi^{(-)}_{1\frac{1}{2}}$	0	2.526
6	4917.0	$00^00^2\Pi_{0\frac{1}{2}}$	$12^00^2\Pi^{(+)}_{0\frac{1}{2}}$	0.018	2.539
7	4929.3	$00^00^2\Pi_{1\frac{1}{2}}$	$20^00^2\Pi_{1\frac{1}{2}}$	0	2.514
2	4932.5	$00^00^2\Pi_{1\frac{1}{2}}$	$04^20^2\Pi^{(+)}_{1\frac{1}{2}}$	0	2.513
7	4941.3	$00^00^2\Pi_{0\frac{1}{2}}$	$20^00^2\Pi_{0\frac{1}{2}}$	0.018	2.526
4	4955.9	$00^00^2\Pi_{0\frac{1}{2}}$	$12^20^2\Pi^{(-)}_{0\frac{1}{2}}$	0.018	2.519
5	4965.4	$00^00^2\Pi_{1\frac{1}{2}}$	$04^00^2\Pi^{(-)}_{1\frac{1}{2}}$	0	2.495
5	4973.6	$00^00^2\Pi_{0\frac{1}{2}}$	$04^00^2\Pi^{(+)}_{0\frac{1}{2}}$	0.018	2.509
2	4997.5	$00^00^2\Pi_{0\frac{1}{2}}$	$04^20^2\Pi^{(-)}_{0\frac{1}{2}}$	0.018	2.499
0	5118.7	$01^10^2\Sigma^{(+)}$	$11^10^2\Sigma^{(-)}$	0.052	2.473
2	5127.7	$02^20^2\Pi^{(-)}_{0\frac{1}{2}}$	$12^20^2\Pi^{(-)}_{0\frac{1}{2}}$	0.102	2.519
5	5144.6	$01^10^2\Sigma^{(+)}$	$11^10^2\Sigma^{(+)}$	0.052	2.460
5	5145.9				
5	5156.3	$01^10^2\Delta_{2\frac{1}{2}}$	$11^10^2\Delta_{2\frac{1}{2}}$	0.057	2.460

APPENDIX IC (Continued)

Intensity	Band Head Wavelengths (in Å)	Spectral Term Symbols and Vib. Quantum Numbers Lower (X)	Upper (A)	Energy Levels (in ev) Lower	Upper
4	5157.7	$00^00^2\Pi_{1\frac{1}{2}}$	$02^20^2\Pi_{1\frac{1}{2}}$	0	2.403
4	5166.1	$01^10^2\Delta_{1\frac{1}{2}}$	$11^10^2\Delta_{1\frac{1}{2}}$	0.075	2.473
8	5168.8	$00^00^2\Pi_{1\frac{1}{2}}$	$10^00^2\Pi_{1\frac{1}{2}}$	0	2.396
8	5180.7	$00^00^2\Pi_{0\frac{1}{2}}$	$10^00^2\Pi_{0\frac{1}{2}}$	0.018	2.410
4	5182.5	$01^10^2\Sigma^{(+)}$	$03^10^2\Sigma^{(+)}$	0.052	2.443
4	5183.5				
8	5196.1	$00^00^2\Pi_{1\frac{1}{2}}$	$02^00^2\Pi_{1\frac{1}{2}}$	0	2.368
8	5207.2	$00^00^2\Pi_{0\frac{1}{2}}$	$02^00^2\Pi_{0\frac{1}{2}}$	0.018	2.398
4	5229.0	$00^00^2\Pi_{0\frac{1}{2}}$	$02^22^2\Pi_{0\frac{1}{2}}^{(-)}$	0.018	2.389
2	5403.8	$01^10^2\Sigma^{(+)}$	$01^10^2\Sigma^{(-)}$	0.052	2.345
2	5407.2				
4	5420.7	$02^20^2\Pi_{0\frac{1}{2}}^{(-)}$	$02^20^2\Pi_{0\frac{1}{2}}^{(-)}$	0.102	2.389
6	5436.0	$01^10^2\Sigma^{(+)}$	$01^10^2\Sigma^{(+)}$	0.052	2.332
6	5437.5				
6	5447.1	$01^10^2\Delta_{2\frac{1}{2}}$	$01^10^2\Delta_{2\frac{1}{2}}$	0.057	2.332
10	5456.8	$00^00^2\Pi_{1\frac{1}{2}}$	$00^00^2\Pi_{1\frac{1}{2}}$	0	2.271
4	5460.1	$01^10^2\Delta_{1\frac{1}{2}}$	$01^10^2\Delta_{1\frac{1}{2}}$	0.075	2.344
--	5468.2	$10^00^2\Pi_{0\frac{1}{2}}$	$10^00^2\Pi_{0\frac{1}{2}}$	0.152	2.410
10	5470.9	$00^00^2\Pi_{0\frac{1}{2}}$	$00^00^2\Pi_{0\frac{1}{2}}$	0.018	2.283
1	5766.5	$11^10^2\Sigma^{(+)}$	$01^10^2\Sigma^{(+)}$	0.183	2.332
1	5767.4				
0	5782.3	$11^10^2\Delta_{2\frac{1}{2}}$	$01^10^2\Delta_{2\frac{1}{2}}$	0.188	2.332
5	5790.7	$10^00^2\Pi_{1\frac{1}{2}}$	$00^00^2\Pi_{1\frac{1}{2}}$	0.131	2.271

APPENDIX IC (Continued)

Intensity	Band Head Wavelengths (in Å)	Spectral Term Symbols and Vib. Quantum Numbers Lower	Upper	Energy Levels (in ev) Lower	Upper
3	5805.8	$20^00^2\Pi_{1\frac{1}{2}}$	$10^00^2\Pi_{1\frac{1}{2}}$	0.263	2.396
5	5813.2	$10^00^2\Pi_{0\frac{1}{2}}$	$00^00^2\Pi_{0\frac{1}{2}}$	0.152	2.283
3	5831.9	$20^00^2\Pi_{0\frac{1}{2}}$	$10^00^2\Pi_{0\frac{1}{2}}$	0.285	2.410
2	6171.6	$20^00^2\Pi_{1\frac{1}{2}}$	$00^00^2\Pi_{1\frac{1}{2}}$	0.263	2.271
2	6202.2	$20^00^2\Pi_{0\frac{1}{2}}$	$00^00^2\Pi_{0\frac{1}{2}}$	0.285	2.283
0	6376.6	$00^02^2\Pi_{1\frac{1}{2}}$	$00^00^2\Pi_{1\frac{1}{2}}$	0.328	2.271
--	6396.0	$00^02^2\Pi_{0\frac{1}{2}}$	$00^00^2\Pi_{0\frac{1}{2}}$	0.346	2.283

APPENDIX II - MINOR SPECIES

APPENDIX II - MINOR SPECIES

APPENDIX IIA. WAVELENGTHS AND WAVENUMBERS OF POSSIBLE EXHAUST SPECIES

Species	Visible (Å)	IR (cm^{-1})
B_2	3273	1061
$B(CN)_3$		No IR spectra due to decrease in CN bond order
BH^+	3768R 3792Q 3803R	
BH_2		2650 2430 840
BH_3		2976 2384 1765 802
$B^{11}H_4$		2264 2244 1210 1080
$B^{10}H_4$		2270 2250 1208 1093
BO_2		1322 1070 464
BO_3^{-3}		1300 750 650

APPENDIX IIA (Continued)

Species	Visible (Å)	IR (cm^{-1})	
$B(OH)_2$		3000	1000
		2500	750
		1300	460
		1150	450
		1100	
$B(OH)_4^-$		950	747
		947	533
		754	379
		749	
BeB_2O_4		2045	764
		1418	744
		1306	300
		877	100
		875	
BeH_2		2200	
		1500	
		1300	
Be_2O		1600	
		1100	
		500	
Be_2O_2		1480	760
		1120	630
		920	460
Be_3O_3		1480	990
		1450	730
		1380	610
		1100	320
Be_4O_4		1400	800
		1200	700
		1150	600
		1000	500
		900	400
		850	200

APPENDIX IIA (Continued)

Species	Visible (Å)	IR (cm^{-1})	
Be_5O_5		1400	700
		1200	600
		1100	500
		1000	400
		900	200
		850	
Be_6O_6		1400	750
		1200	700
		1100	600
		1000	500
		950	400
		900	250
		850	200
		800	

	Swan		Muliken				
C_2	4698	5165	U. V.			1856	1641
	4715	5541				1830	1608
	4737	5586				1809	1107
	5129	5636				1788	
C	5794						
	7119						
C^+	3876	6578					
	3921	6583					
	4075	6784					
	4267	7231					
	5145	7236					
CH	4313Q					2816	
CN	Red	Main		Tail			
	6355Q	3584	3883	3405	3629	2164	
	6502Q	3586	4168	3433	3880	2069	
	7874R	3590	4181	3465	3910	1814	
	8067	3855	4197	3603	3945		
	9140R	3862	4216		3985		
	9393	3871					

APPENDIX IIA (Continued)

Species	Visible (Å)		IR (cm^{-1})	
CN^-			2250-2050	
C_2N_2	U. V.		2322	
CO^+			2149	
			2214	
			1734	
H_3BO_3			1562	
			3250	1060
			3150	881
			1440	652
			1185	544
HCN	7880a		3311	
	7912a		2097	
HNCO			712	
			3531	797
			2274	670
			1327	572
HNO			3450	
HNO_2	3417a		trans	cis
	3539a		3426	3590
	3545a		1640	1696
	3680a		1292	1260
			856	794
			637	598
				543
H_2O_2	3700a		3610	1262
			3417	890
			2870	
	Flames	Chemiluminescence		
NH	3360Q	3035R	3300	
	3370Q	3042Q		
		3240R		
		3253Q		
		3610R		
		3627Q		

APPENDIX IIA (Continued)

Species	Visible (Å)		IR (cm^{-1})	
NH_2	4723	5707		
	5166	5708		
	5525	6333		
	5705			
NH_3			N^{14}	N^{15}
			3448	3335
			3414	1625
			3337	961
			1627	926
			968	
			950	
			932	
N_3H			3336	1150
			2140	672
			1274	522
NO	3886		2374	1712
	3801		2371	1380
			2347	1300
			2327	1262
			1904	1170
			1876-N^{14}	1155
			1843-N^{15}	1038
			1748	1037
				1020
			stretch: 2400-900	
			monomer: 1883	
			cis-dimer: 1862, 1768	
			trans-dimer: 1740	
NO^+	6000		2220	

APPENDIX IIA (Continued)

Species	Visible (Å)	IR (cm^{-1})		
		N^{14}		N^{15}
NO_2	4350a	1618	485	1580
	4390a	1318	482	1306
	4448a	808	429	740
	480a	750	381	
	4630a	672	370	
		O-N-O stretch: 900-400		
NO_2^+		2360		
		1400		
		667		
N_2O	Continuous absorption through U. V. to 3065Å	$N^{14}N^{14}O$		$N^{15}N^{15}O$
		2224		2178
		1286		1281
		589		576
		$N^{15}N^{14}O$		$N^{15}N^{15}O$
		2203		2156
		1271		1266
		586		572

APPENDIX IIB. VISIBLE COINCIDENCE TABLE

Å

3035R - NH
3042Q - NH
3065a - N_2O
3240R - NH
3253Q - NH
3273 - B_2
3360Q - NH
3370Q - NH
3386 - NO
3405 - CN
3417a - HNO_2
3433 - CN
3465 - CN
3539a - HNO_2
3545a - HNO_2
3584 - NO, CN
3586 - CN
3590 - CN
3603 - CN
3610R - NH
3627Q - NH
3629 - CN
3680a - HNO_2
3700a - H_2O_2
3768R - BH^+
3792Q - BH^+
3801 - NO
3803R - BH^+
3855 - CN
3862 - CN
3871 - CN
3876 - C+
3880 - CN
3883 - CN
3910 - CN
3921 - C^+
3945 - CN
3985 - CN
4075 - C^+
4168 - CN
4181 - CN
4197 - CN
4216 - CN
4267 - C^+
4313Q - CH
4350 - NO_2
4390a - NO_2
4448a - NO_2
4480a - NO_2
4630a - NO_2
4698 - C_2
4715 - C_2
4723 - NH_2
4737 - C_2
5129 - C_2
5145 - C^+
5165 - C_2
5166 - NH_2
5525 - NH_2
5541 - C_2
5586 - C_2
5636 - C_2
5705 - NH_2
5707 - NH_2
5708 - NH_2
5794 - C
6000 - NO^+
6333 - NH_2
6355Q - CN
6502Q - CN
6578 - C^+
6583 - C^+
6784 - C^+
7119 - C
7231 - C^+
7236 - C^+
7874R - CN
7880a - HCN
7912a - HCN
8067 - CN
9140R - CN
9393 - CN

(a) - absorption
(Q) - Q branch
(R) - R branch

APPENDIX IIB (Continued)

INFRARED COINCIDENCE TABLE

cm^{-1}

3610 - H_2O_2
3590 - HN_3
3531 - HNCO
3450 - HNO
3448 - NH_3
3426 - HNO_2
3417 - H_2O_2
3414 - NH_3
3337 - NH_3
3336 - N_3H
3335 - NH_3
3311 - HCN
3300 - NH
3250 - H_3BO_3
3150 - H_3BO_3
3000 - $B(OH)_2$
2976 - BH_3
2870 - H_2O_2
2816 - CH
2650 - BH_2
2500 - $B(OH)_2$
2430 - BH_2
2384 - BH_3
2374 - NO
2371 - NO
2360 - NO_2^+
2347 - NO
2327 - NO
2322 - C_2N_2
2274 - HNCO
2270 - $B^{10}H_4$
2264 - $B^{11}H_4$
2250 - $B^{10}H_4$
2244 - $B^{11}H_4$
2224 - N_2O
2214 - CO^+

2203 - N_2O
2200 - BeH_2, NO^+
2178 - N_2O CN^-
2164 - CN
2156 - N_2O
2149 - C_2N_2
2140 - N_3H
2097 - HCN
2069 - CN
2045 - BeB_2O_4
1904 - NO
1876 - NO
1856 - C_2
1843 - NO
1830 - C_2
1814 - CN
1809 - C_2
1788 - C_2
1765 - BH_3
1748 - NO
1734 - CO^+
1712 - NO
1696 - HNO_2
1640 - HNO_2
1627 - NH_3
1625 - NH_3
1618 - NO_2
1608 - C_2
1600 - Be_2O
1580 - NO_2
1562 - CO^+
1500 - BeH_2
1480 - Be_2O_2, Be_3O_3
1450 - Be_3O_3
1440 - H_3BO_3
1418 - BeB_2O_4

1400 - $Be_4O_4Be_5O_5, Be_6O_6, NO_2^+$
1380 - Be_3O_3, NO
1327 - HNCO
1322 - BO_2
1318 - NO_2
1306 - BeB_2O_4, NO_2
1300 - BeH_2, NO, BO_3^{-3}, $B(OH)_2$
1292 - HNO_2
1286 - N_2O
1281 - N_2O
1274 - N_3H
1271 - N_2O
1262 - H_2O_2, NO
1260 - HNO_2, N_2O
1210 - $B^{11}H_4$
1208 - $B^{10}H_4$
1200 - Be_4O_4, Be_5O_5, Be_6O_6
1185 - H_3BO_3
1170 - NO
1155 - NO
1150 - H_3H, $B(OH)_2$, $B[illegible]O_4$
1120 - Be_2O_2
1107 - C_2
1100 - $B(OH)_2$, Be_2O, Be_3O_3, Be_5O_5, Be_6O_6
1093 - $B^{10}H_4$
1080 - $B^{11}H_4$
1070 - BO_2
1061 - B_2
1060 - H_3BO_3
1038 - NO
1037 - NO
1020 - NO
1000 - $B(OH)_2$, Be_4O_4, Be_5O_5, Be_6O_6
990 - Be_3O_3
968 - NH_3
961 - NH_3
950 - $B(OH)_4NH_3$
947 - $B(OH)_4$
932 - NH_3
926 - NH_3
920 - Be_2O_2
900 - Be_4O_4, Be_5O_5, Be_6O_6
890 - H_2O_2
881 - H_3BO_3
877 - BeB_2O_4
875 - BeB_2O_4
856 - HNO_2
850 - Be_4O_4, Be_5O_5, Be_6O_6
840 - BH_3
808 - NO_2
802 - BH_3
800 - Be_4O_4, Be_6O_6
797 - HNCO
794 - HNO_2
764 - BeB_2O_4
760 - Be_2O_2
754 - $B(OH)_4$
750 - NO_2, BO_3^{-3}, Be_5O_6, $B(OH)_2$
749 - $B(OH)_4^-$
747 - $B(OH)_4^-$
744 - BeB_2O_4
740 - NO_2
730 - Be_3O_3
712 - HCN
700 - Be_4O_4, Be_5O_5, Be_6O_6
672 - N_3H, NO_2
670 - HNCO
667 - NO_2^+
652 - H_3BO_3
650 - BO_3^{-3}
637 - HNO_2
630 - Be_2O_2
610 - Be_3O_3
600 - Be_4O_4, Be_5O_5, Be_6O_6
598 - HNO_2
589 - N_2O
586 - N_2O
575 - N_2O

APPENDIX III

APPENDIX III. OBSERVATIONS AND COMMENTS RELATED TO SAFETY AND HANDLING CHARACTERISTICS OF HYBALINE B-3

The toxicity of Hybaline B-3 was expected to be quite high. Therefore all test operations used the appropriate safety procedures and equipment necessary for beryllium handling. All operations were carried out either out-of-doors or in specially protected enclosed rooms having a positive one micron filter on all air exhaust fans and vents.

A number of observations were made regarding the handling of this compound during the course of these studies. Previous workers, with the exception of personnel at Edwards AFB, have reported that Hybaline B-3 is not pyrophoric. On this program pyrophoric behavior was observed on a number of occasions. These occurred either upon drawing from the main storage tank or in open transfer operations where humid conditions prevailed. Maximum danger of fire occurred when drawing from the main storage tank after a long inactive period. It is assumed that the cause of pyrophoricity is diborane formed in a slow decomposition of the neat propellant. Therefore, dry nitrogen and/or inert gases such as argon or helium are recommended for purging in all transfer procedures, and use of an inert gas blanket is strongly advised during storage.

In addition to the pyrophoric behavior, a second problem arose during spills or disposal of neat propellant on the ground. A sporadically delayed, violet reaction which closely resembled a detonation, occurred some period of time after ground contact had been made. It is therefore recommended that caution be exercised any time a ground spill or disposal occurs.

On several occasions an explosion occurred when the neat propellant came into contact with the residue remaining when the propellant had been allowed to evaporate. These explosions were infrequent, but sufficiently strong to shatter glass beakers and watch glasses.

The use of air packs is strongly suggested for personnel protection during the handling of this propellant. The use of hydrazine gas masks is not recommended since the smell of Hybaline B-3 can be detected through such equipment. The odor of this propellant was detected by two personnel on separate occasions and was reported as

"sweet" and "similar to dandelions." Both personnel agreed that the odor was pleasant although somewhat faint. The color of the Hybaline B-3 was observed to be quite dark green, or black and ink like in appearance.

No problem of materials compatibility was observed and common materials of constructure were used for all handling and storage equipment. The use of polyethylene hose connections was satisfactory. Rubber absorbs the liquid and is therefore not recommended.

DISTRIBUTION LIST

No. of Copies	Recipient
2	AFRPL (RPCL) Edwards, California 93523
1	RTD (RTTA) Bolling AFB, Washington, D.C. 20332
1	U. S. Department of the Interior Bureau of Mines 4800 Forbes Avenue Pittsburgh, Pennsylvania 15213 Attn: M. M. Dolinar, Repts Librarian Explosives Research Center
1	Central Intelligence Agency 2430 E. Street, N. W. Washington, D. C. 20505 Attn: OCD, Standard Dist.
1	Office of the Director of Defense Research and Engineering Washington, D. C. 20301 Attn: Dr. H. W. Schulz, Office of Asst. Dir. (Chem. Technology)
1	Nat'l Aeronautics & Space Admin. Lewis Research Center 21000 Brookpark Road Cleveland, Ohio 44135 Attn: Library
1	John F. Kennedy Space Center NASA Cocoa Beach, Florida 32931 Attn: Library
1	Nat'l Aeronautics & Space Admin. Manned Spacecraft Center P. O. Box 1537 Houston, Texas 77001 Attn: Library

Unclassified
Security Classification

DOCUMENT CONTROL DATA - R&D

(Security classification of title, body of abstract and indexing annotation must be entered when the overall report is classified)

1. ORIGINATING ACTIVITY (Corporate author)
Denver Research Institute
University of Denver
(Colorado Seminary)

2a. REPORT SECURITY CLASSIFICATION

2b. GROUP

3. REPORT TITLE
"Spectrometric Evaluation of Metal Containing Fuels"

4. DESCRIPTIVE NOTES (Type of report and inclusive dates)
Final and Summary Technical Report (June 1965 - June 1966)

5. AUTHOR(S) (Last name, first name, initial)
McLain, William H. and Evans, Robert W.

6. REPORT DATE
July 1967

7a. TOTAL NO. OF PAGES
100

7b. NO. OF REFS
23

8a. CONTRACT OR GRANT NO.
AF 04(611)-10782

b. PROJECT NO.
3148

c.

d.

9a. ORIGINATOR'S REPORT NUMBER(S)
558-6608-F

9b. OTHER REPORT NO(S) (Any other numbers that may be assigned this report)

10. AVAILABILITY/LIMITATION NOTICES
Qualified requesters may obtain copies of this report from DDC

11. SUPPLEMENTARY NOTES

12. SPONSORING MILITARY ACTIVITY
Air Force Flight Test Center
(FTMKR-3) Edwards Air Force Base
California

13. ABSTRACT

The spectral characteristics of high temperature Hybaline B-3 fueled combustion reactions are reported. Data were obtained for Hybaline B-3 augmented hydrogen-oxygen, deuterium-oxygen, acetylene-oxygen, and air diffusion flames under conditions simulating rocket test firings. Major features of the emission spectra are outlined for the ultraviolet, visible, and infrared regions. Sufficient specific emission is available to indicate the feasibility of determining changes in the species concentrations and flame temperatures as functions of changes in O/F ratios and other major rocket parameters.

DD FORM 1 JAN 64 1473

Unclassified
Security Classification

Unclassified

Security Classification

14. KEY WORDS	LINK A ROLE	LINK A WT	LINK B ROLE	LINK B WT	LINK C ROLE	LINK C WT
Hybaline B-3						
Spectra, Infrared						
Spectra, Visible						
Spectra, Ultraviolet						
Propellant, liquid						
Combustion, rocket fuels						
Pyrolysis products						

INSTRUCTIONS

1. ORIGINATING ACTIVITY: Enter the name and address of the contractor, subcontractor, grantee, Department of Defense activity or other organization *(corporate author)* issuing the report.

2a. REPORT SECURITY CLASSIFICATION: Enter the overall security classification of the report. Indicate whether "Restricted Data" is included. Marking is to be in accordance with appropriate security regulations.

2b. GROUP: Automatic downgrading is specified in DoD Directive 5200.10 and Armed Forces Industrial Manual. Enter the group number. Also, when applicable, show that optional markings have been used for Group 3 and Group 4 as authorized.

3. REPORT TITLE: Enter the complete report title in all capital letters. Titles in all cases should be unclassified. If a meaningful title cannot be selected without classification, show title classification in all capitals in parenthesis immediately following the title.

4. DESCRIPTIVE NOTES: If appropriate, enter the type of report, e.g., interim, progress, summary, annual, or final. Give the inclusive dates when a specific reporting period is covered.

5. AUTHOR(S): Enter the name(s) of author(s) as shown on or in the report. Enter last name, first name, middle initial. If military, show rank and branch of service. The name of the principal author is an absolute minimum requirement.

6. REPORT DATE: Enter the date of the report as day, month, year; or month, year. If more than one date appears on the report, use date of publication.

7a. TOTAL NUMBER OF PAGES: The total page count should follow normal pagination procedures, i.e., enter the number of pages containing information.

7b. NUMBER OF REFERENCES: Enter the total number of references cited in the report.

8a. CONTRACT OR GRANT NUMBER: If appropriate, enter the applicable number of the contract or grant under which the report was written.

8b, 8c, & 8d. PROJECT NUMBER: Enter the appropriate military department identification, such as project number, subproject number, system numbers, task number, etc.

9a. ORIGINATOR'S REPORT NUMBER(S): Enter the official report number by which the document will be identified and controlled by the originating activity. This number must be unique to this report.

9b. OTHER REPORT NUMBER(S): If the report has been assigned any other report numbers *(either by the originator or by the sponsor)*, also enter this number(s).

10. AVAILABILITY/LIMITATION NOTICES: Enter any limitations on further dissemination of the report, other than those imposed by security classification, using standard statements such as:

(1) "Qualified requesters may obtain copies of this report from DDC."

(2) "Foreign announcement and dissemination of this report by DDC is not authorized."

(3) "U. S. Government agencies may obtain copies of this report directly from DDC. Other qualified DDC users shall request through _____."

(4) "U. S. military agencies may obtain copies of this report directly from DDC. Other qualified users shall request through _____."

(5) "All distribution of this report is controlled. Qualified DDC users shall request through _____."

If the report has been furnished to the Office of Technical Services, Department of Commerce, for sale to the public, indicate this fact and enter the price, if known.

11. SUPPLEMENTARY NOTES: Use for additional explanatory notes.

12. SPONSORING MILITARY ACTIVITY: Enter the name of the departmental project office or laboratory sponsoring *(paying for)* the research and development. Include address.

13. ABSTRACT: Enter an abstract giving a brief and factual summary of the document indicative of the report, even though it may also appear elsewhere in the body of the technical report. If additional space is required, a continuation sheet shall be attached.

It is highly desirable that the abstract of classified reports be unclassified. Each paragraph of the abstract shall end with an indication of the military security classification of the information in the paragraph, represented as *(TS)*, *(S)*, *(C)*, or *(U)*.

There is no limitation on the length of the abstract. However, the suggested length is from 150 to 225 words.

14. KEY WORDS: Key words are technically meaningful terms or short phrases that characterize a report and may be used as index entries for cataloging the report. Key words must be selected so that no security classification is required. Identifiers, such as equipment model designation, trade name, military project code name, geographic location, may be used as key words but will be followed by an indication of technical context. The assignment of links, rules, and weights is optional.

SUPPLEMENTARY

INFORMATION

AD-816 133

ADDENDUM

Report Number AFRPL-TR-67-132 was omitted from final report distributed under Contract AF 04(611)-10782.